



U.S. DEPARTMENT OF
ENERGY

Office of
Science

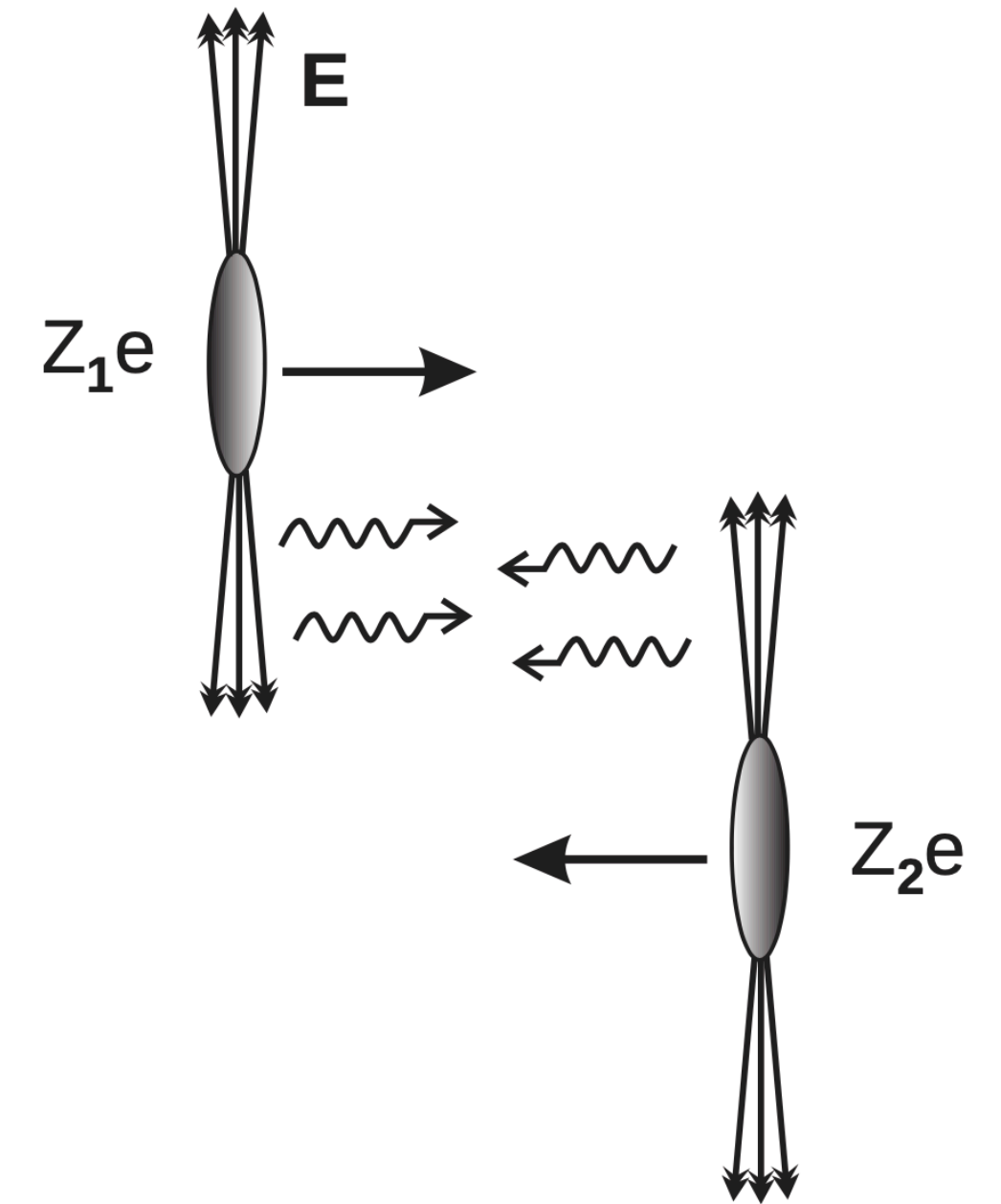
NUCLEAR GEOMETRY IN ULTRA-PERIPHERAL COLLISIONS

BJÖRN SCHENKE, BROOKHAVEN NATIONAL LABORATORY

Light Ion Collisions at the LHC
CERN
11/12/2024

Ultrapерipheral collisions (UPC)

- At an impact parameter $|b_T| > 2R_A$ nuclei are photon sources
- Photons are quasi-real $Q^2 \lesssim 1/R_A^2$
- High energy $\gamma + \gamma, \gamma + p, \gamma + A$ at RHIC and LHC
- Consider exclusive vector meson production: Ignoring interference, the cross section is a convolution of photon flux n^{A_1} from nucleus A_1 and the γA_2 cross section (and vice versa):



$$\frac{d\sigma^{AA \rightarrow VAA'}}{dt} = n^{A_2}(\omega_2) \sigma_{\gamma A_1 \rightarrow VA'_1}(y) + n^{A_1}(\omega_1) \sigma_{\gamma A_2 \rightarrow VA'_2}(-y)$$

y is the rapidity of the VM and photon energies are $\omega_1 = (M_V/2)e^y, \omega_2 = (M_V/2)e^{-y}$

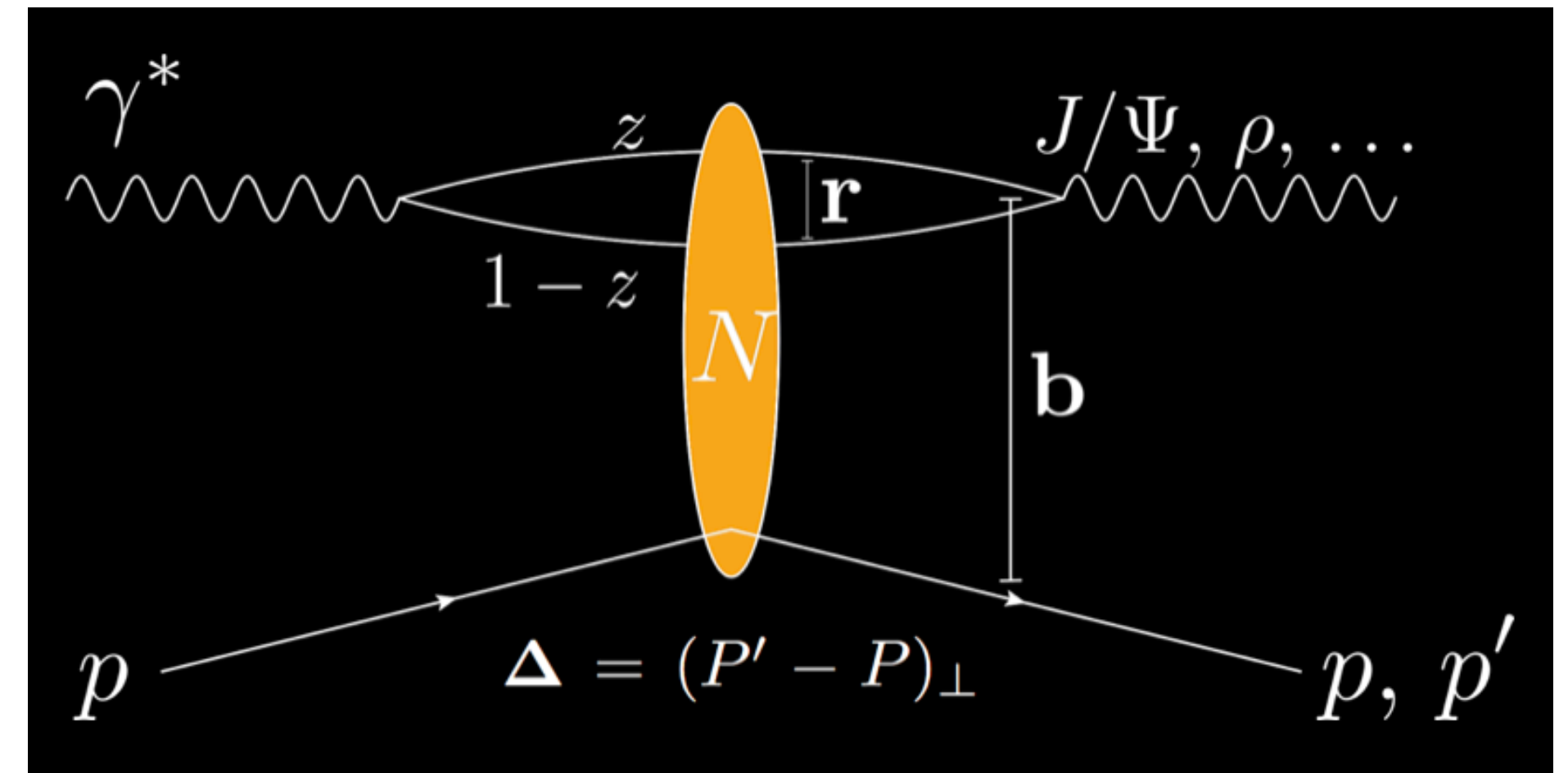
- Interference is important for the differential cross-section in A+A, especially at midrapidity

Vector meson production - Dipole picture

H. Mäntysaari, B. Schenke, Phys. Rev. Lett. 117 (2016) 052301; Phys.Rev. D94 (2016) 034042

High energy factorization:

- $\gamma^* \rightarrow q\bar{q} : \psi^\gamma(r, Q^2, z)$
- $q\bar{q}$ dipole scatters with amplitude N
- $q\bar{q} \rightarrow V : \psi^V(r, Q^2, z)$



$$A \sim \int d^2b dz d^2r \psi^* \psi^V(\vec{r}, z, Q^2) e^{-i(\vec{b} - (\frac{1}{2} - z)\vec{r}) \cdot \vec{\Delta}} N(\vec{r}, x, \vec{b})$$

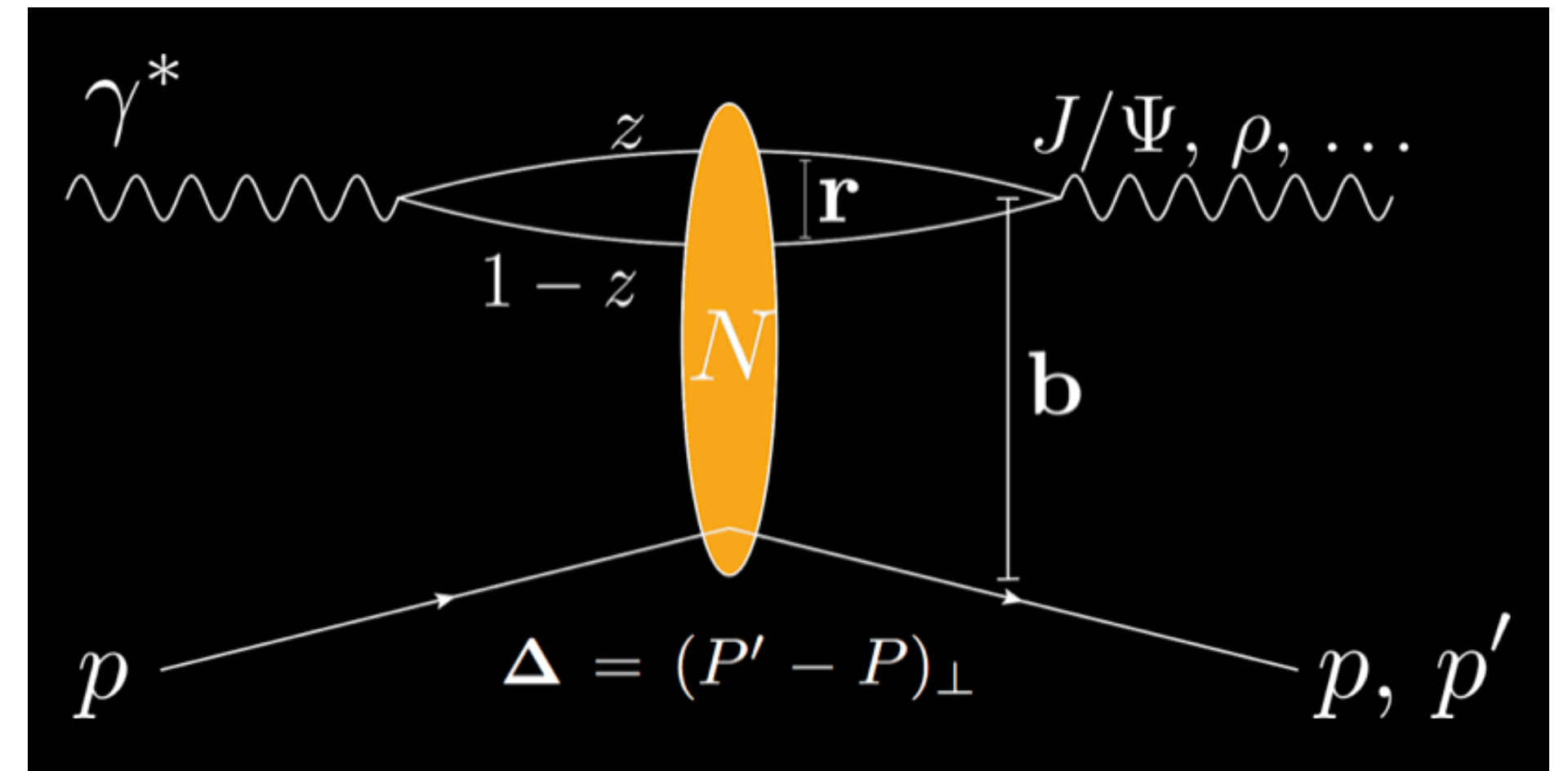
- Impact parameter \mathbf{b} is the Fourier conjugate of transverse momentum transfer $\mathbf{\Delta}$:
Access to spatial structure ($t = -\Delta^2$)

Color Glass Condensate Formalism

H. Mäntysaari, B. Schenke, Phys. Rev. Lett. 117 (2016) 052301; Phys.Rev. D94 (2016) 034042

$$\begin{aligned}
 N(\vec{r}, x, \vec{b}) &= N(\vec{x} - \vec{y}, x, (\vec{x} + \vec{y})/2) \\
 &= 1 - \text{Tr}(\mathbf{V}(\vec{x})\mathbf{V}^\dagger(\vec{y}))/N_c
 \end{aligned}$$

The trace appears at the level of the amplitude, because we project on a **color singlet**:
Exclusive vector meson production



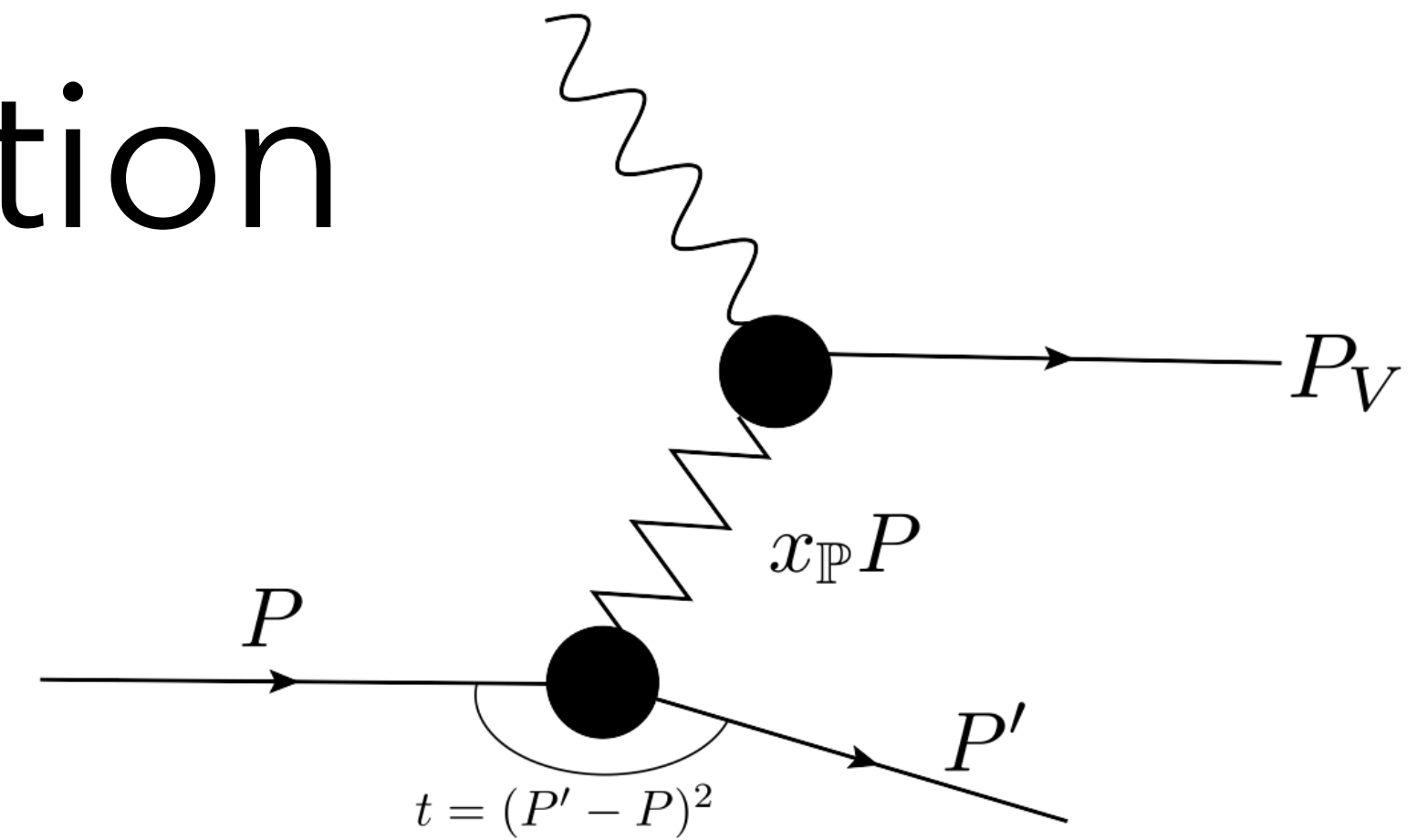
Compute the Wilson lines using color charges whose correlator depends on \vec{b}_\perp (for example using MV model with impact parameter dependence):

$$\langle \rho^a(\mathbf{b}_\perp)\rho^b(\mathbf{x}_\perp) \rangle = g^2 \mu^2(x, \mathbf{b}_\perp) \delta^{ab} \delta^{(2)}(\mathbf{b}_\perp - \mathbf{x}_\perp)$$

Diffractive Vector Meson Production

— Coherent diffraction:
$$\frac{d\sigma^{\gamma^*p \rightarrow Vp}}{dt} = \frac{1}{16\pi} \left| \left\langle A^{\gamma^*p \rightarrow Vp} \left(x_P, Q^2, \vec{\Delta} \right) \right\rangle \right|^2$$

sensitive to the average size of the target



— Incoherent diffraction:
$$\frac{d\sigma^{\gamma^*p \rightarrow Vp^*}}{dt} = \frac{1}{16\pi} \left(\left\langle \left| A^{\gamma^*p \rightarrow Vp} \left(x_P, Q^2, \vec{\Delta} \right) \right|^2 \right\rangle - \left| \left\langle A^{\gamma^*p \rightarrow Vp} \left(x_P, Q^2, \vec{\Delta} \right) \right\rangle \right|^2 \right)$$

sensitive to fluctuations (including geometric ones)

H. Kowalski, L. Motyka, G. Watt, Phys.Rev. D 74 (2006) 074016

A. Caldwell, H. Kowalski, EDS 09, 190-192, e-Print: 0909.1254 [hep-ph]

M. L. Good and W. D. Walker, Phys. Rev. 120 (1960) 1857

H. I. Miettinen and J. Pumplin, Phys. Rev. D18 (1978) 1696

Y. V. Kovchegov and L. D. McLerran, Phys. Rev. D60 (1999) 054025

A. Kovner and U. A. Wiedemann, Phys. Rev. D64 (2001) 114002

Model impact parameter dependence (in nucleons)

H. Mäntysaari, B. Schenke, Phys. Rev. Lett. 117 (2016) 052301; Phys.Rev. D94 (2016) 034042

1) Assume Gaussian proton shape:

$$T(\vec{b}) = T_p(\vec{b}) = \frac{1}{2\pi B_p} e^{-b^2/(2B_p)}$$

2) Assume a substructure of the nucleon. For example Gaussian distributed and Gaussian shaped hot spots:

$$P(b_i) = \frac{1}{2\pi B_{qc}} e^{-b_i^2/(2B_{qc})} \quad (\text{angles uniformly distributed})$$

$$T_p(\vec{b}) = \frac{1}{N_q} \sum_{i=1}^{N_q} T_q(\vec{b} - \vec{b}_i) \quad \text{with } N_q \text{ hot spots;} \quad T_q(\vec{b}) = \frac{1}{2\pi B_q} e^{-b^2/(2B_q)}$$

Diffractive J/ψ production in $e+p$ at HERA

Nucleon parameters $B_{q'}$, $B_{qc'}$ can be constrained by $e+p$ scattering data from HERA

Exclusive diffractive J/ψ production in $e+p$:

Incoherent x-sec sensitive to fluctuations

H. Mäntysaari, B. Schenke, Phys. Rev. Lett. 117 (2016) 052301

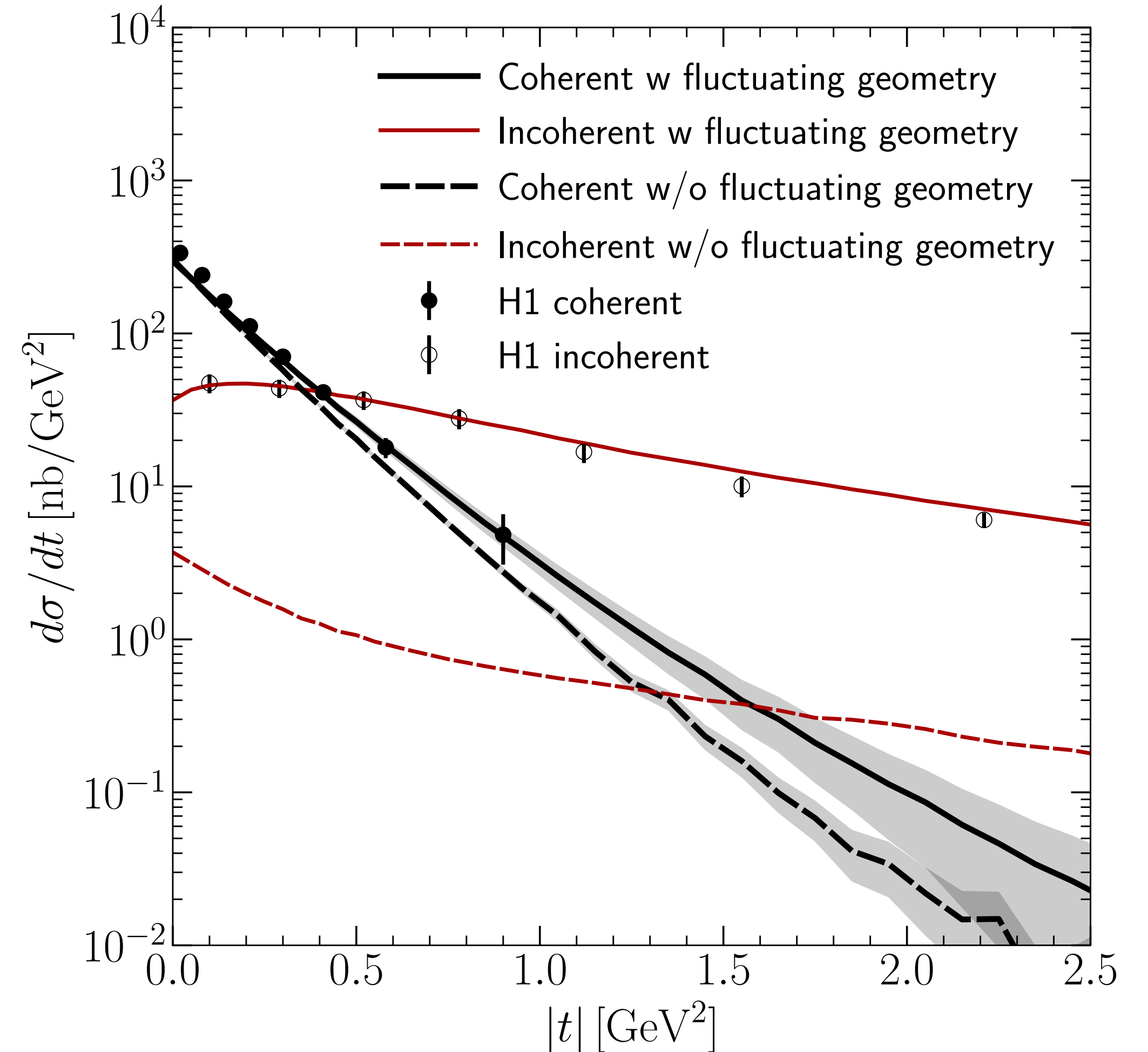
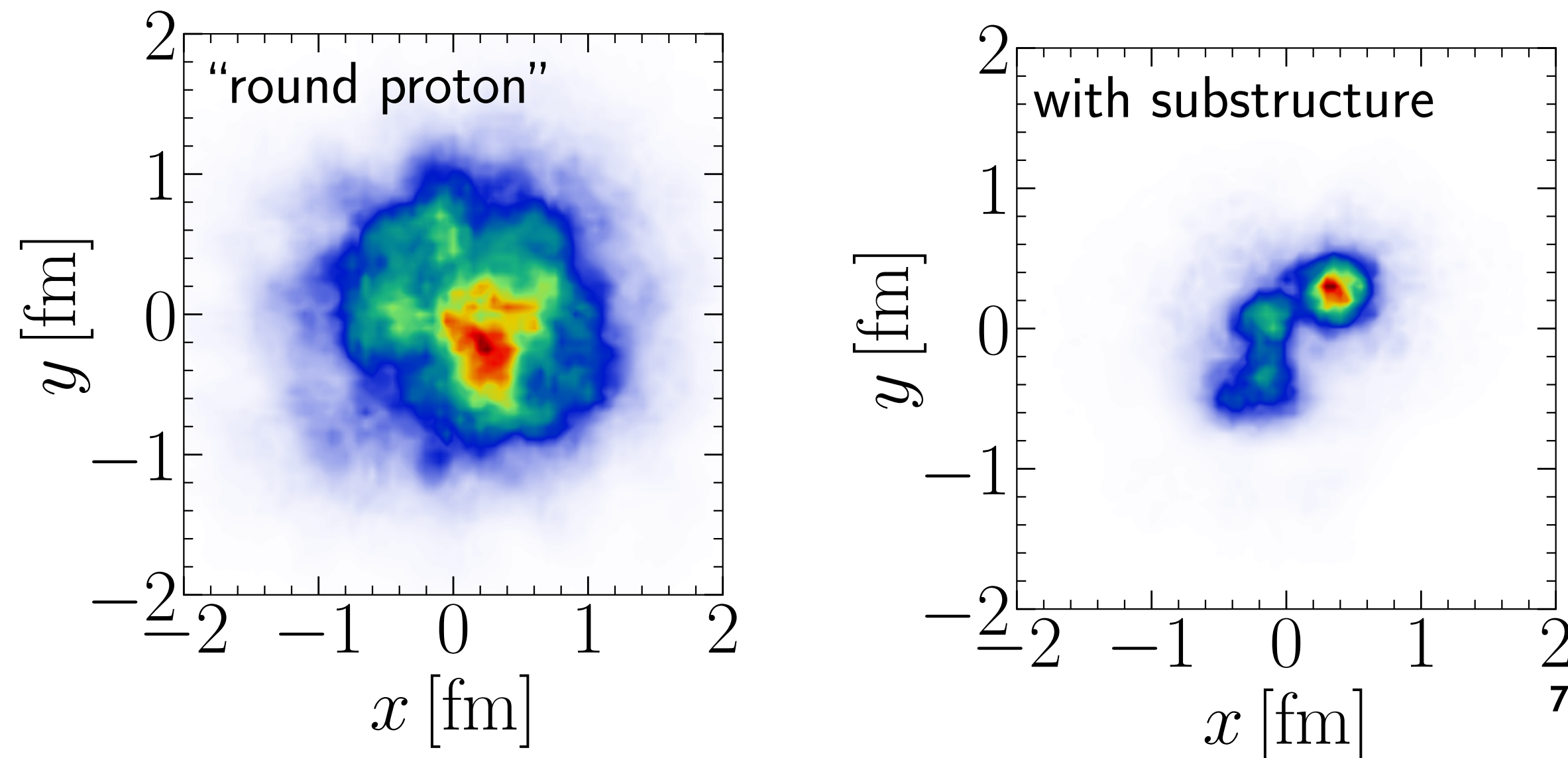
Phys.Rev. D94 (2016) 034042

also see:

S. Schlichting, B. Schenke, Phys.Lett. B739 (2014) 313-319

H. Mäntysaari, Rep. Prog. Phys. 83 082201 (2020)

B. Schenke, Rep. Prog. Phys. 84 082301 (2021)



H1 Collaboration, Eur. Phys. J. C73 (2013) no. 6 2466

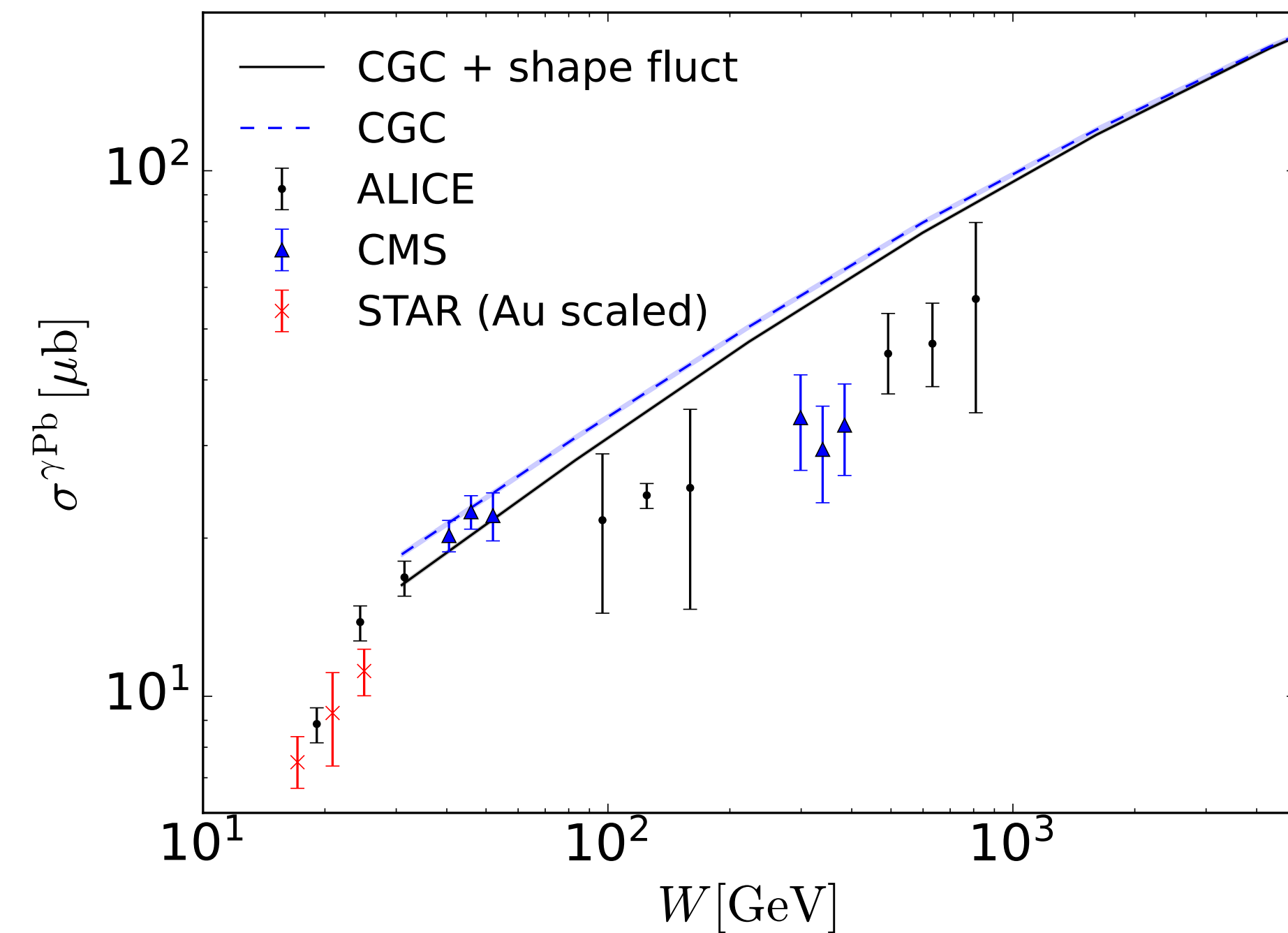
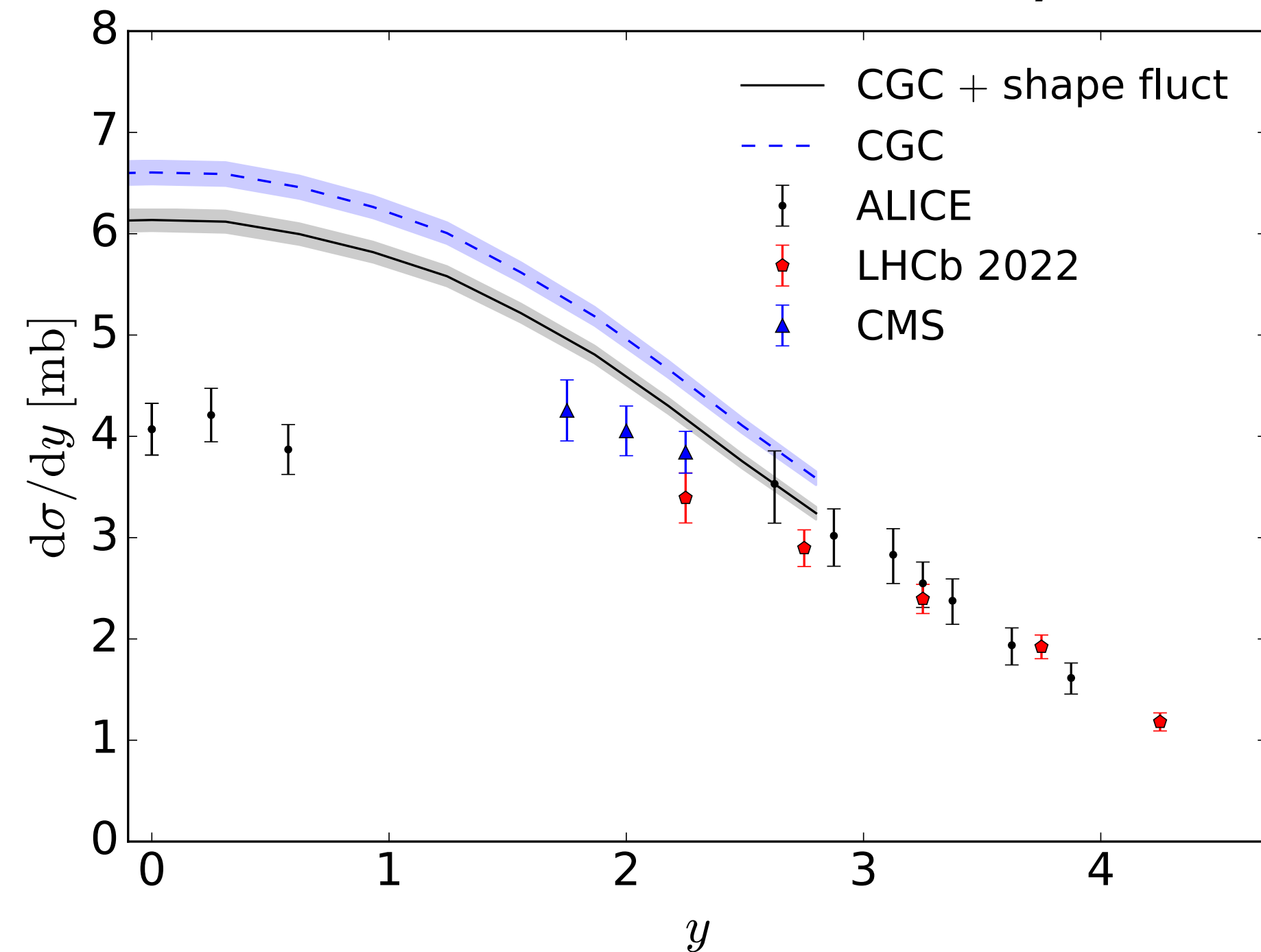
Back to UPCs: Coherent cross section

H. Mäntysaari, F. Salazar, B. Schenke, *Phys.Rev.D* 106 (2022) 7, 074019 and [arXiv:2312.04194](https://arxiv.org/abs/2312.04194)

Calculation is constrained by HERA J/ψ production data

$$\text{Pb+Pb} \rightarrow \text{Pb+Pb+}J/\psi$$

$$\gamma+\text{Pb} \rightarrow J/\psi + \text{Pb}$$



Larger suppression when including shape fluctuations: Hotter hot spots; larger local Q_s

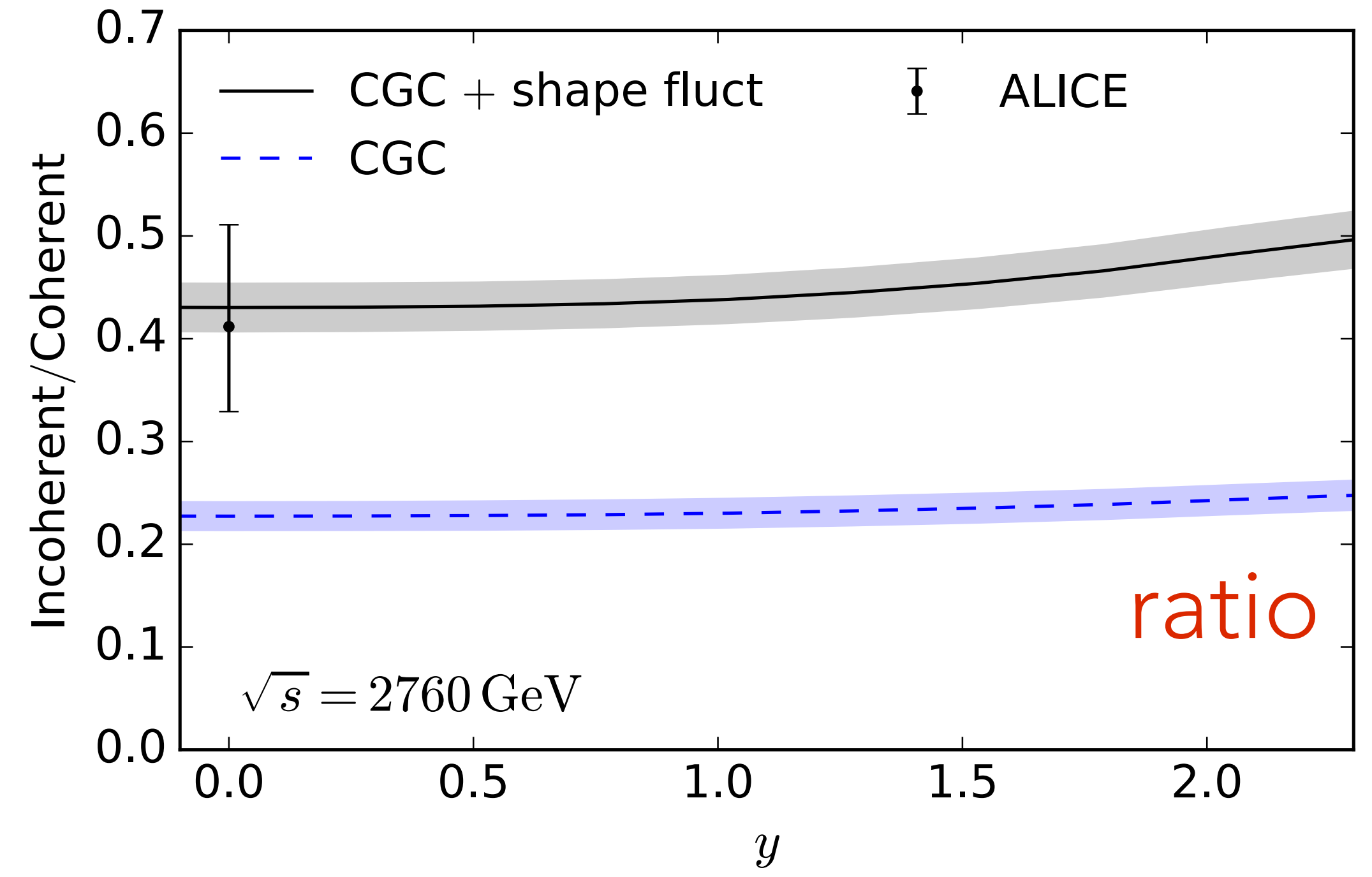
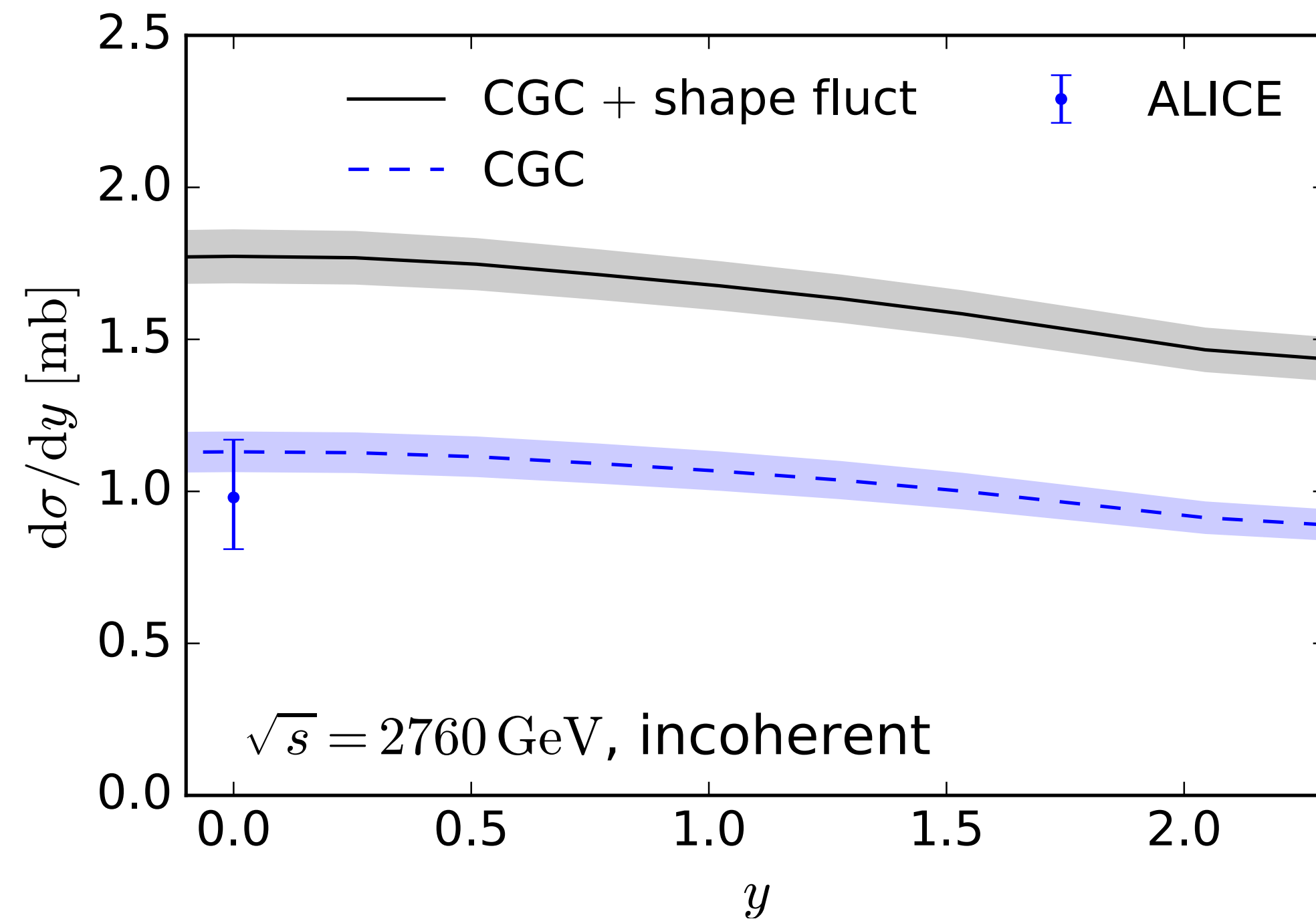
ALICE Collaboration, S. Acharya et. al., *Eur. Phys. J. C*81 (2021) no. 8 712 [[arXiv:2101.04577](https://arxiv.org/abs/2101.04577)]

CMS Collaboration, A. Tumasyan et. al., [arXiv:2303.16984](https://arxiv.org/abs/2303.16984)

LHCb Collaboration, R. Aaij et. al., *JHEP* 06 146 (2023) [[arXiv:2206.08221](https://arxiv.org/abs/2206.08221)]

Incoherent cross section

H. Mäntysaari, F. Salazar, B. Schenke, Phys.Rev.D 106 (2022) 7, 074019

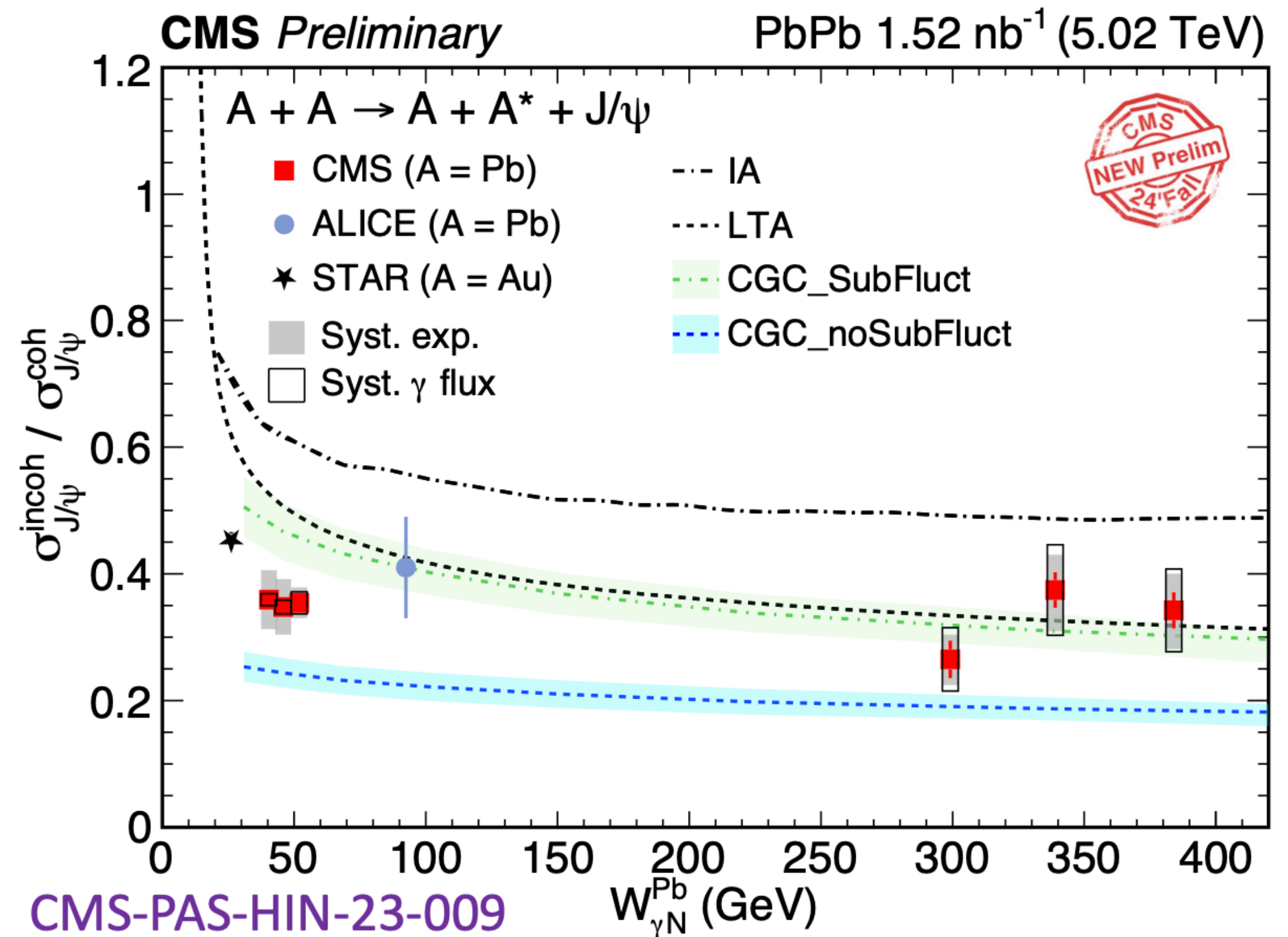
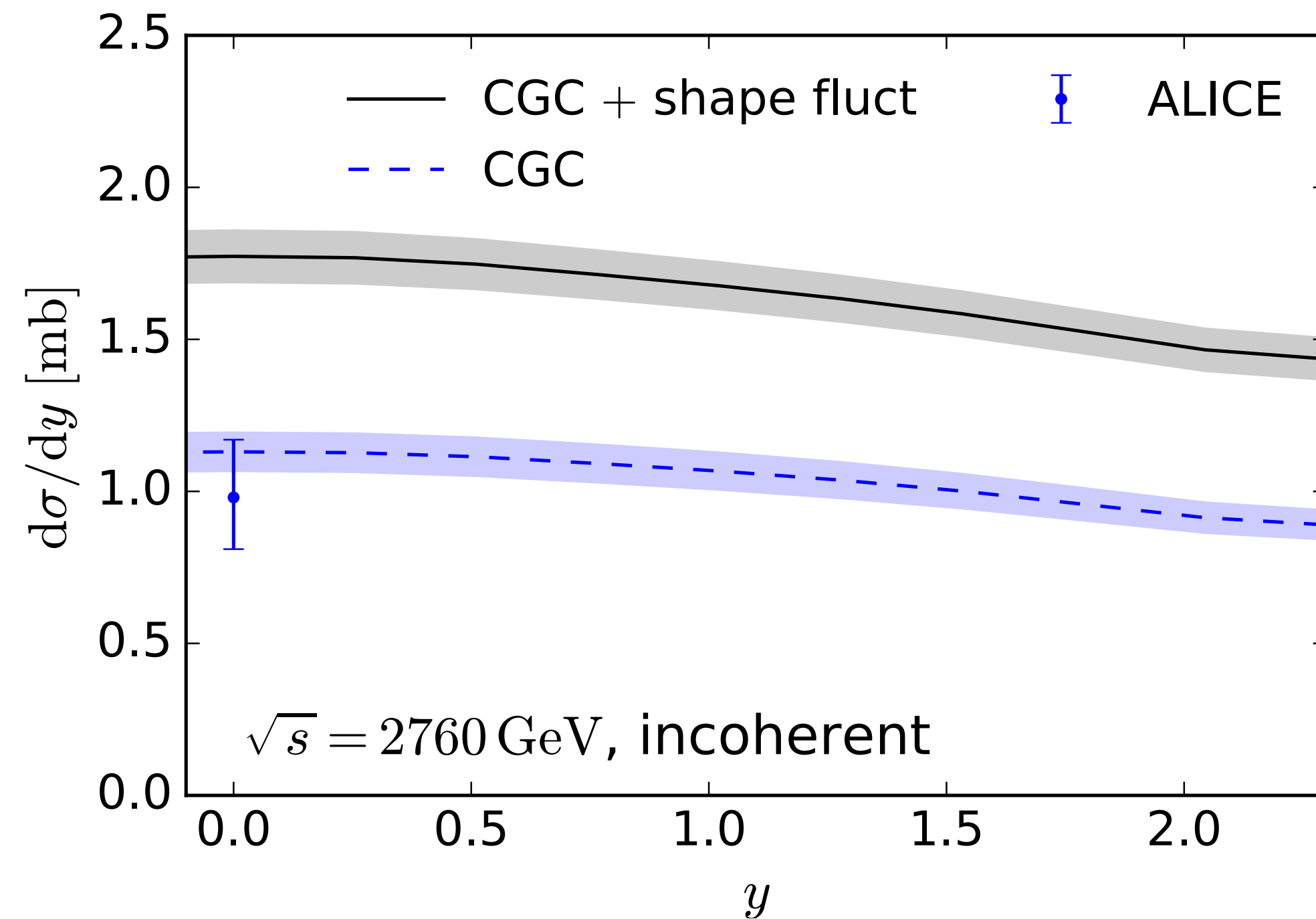


More fluctuations when including shape fluctuations → larger incoherent cross section
Ratio of coherent to incoherent well described (both coh. and incoh. overestimated)

ALICE Eur. Phys. J. C73 (2013) no. 11 2617

Incoherent cross section

H. Mäntysaari, F. Salazar, B. Schenke, Phys.Rev.D 106 (2022) 7, 074019



new CMS results shown at Hard Probes 2024
CMS-PAS-HIN-23-009

More fluctuations when including shape fluctuations → larger incoherent cross section
Ratio of coherent to incoherent well described (both coh. and incoh. overestimated)

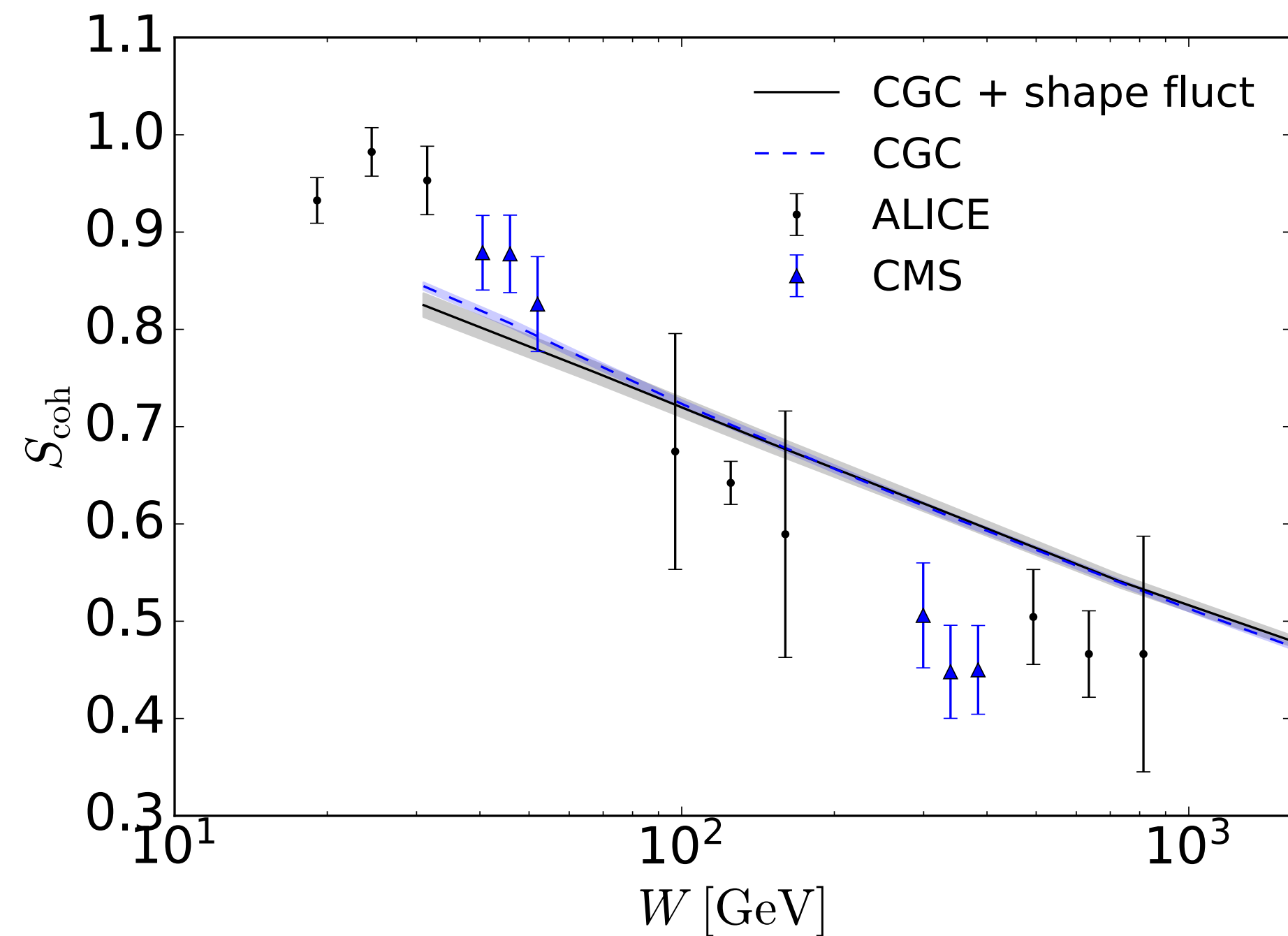
ALICE Eur. Phys. J. C73 (2013) no. 11 2617

Nuclear suppression

H. Mäntysaari, F. Salazar, B. Schenke, Phys. Rev. D 109, L071504 (2024)

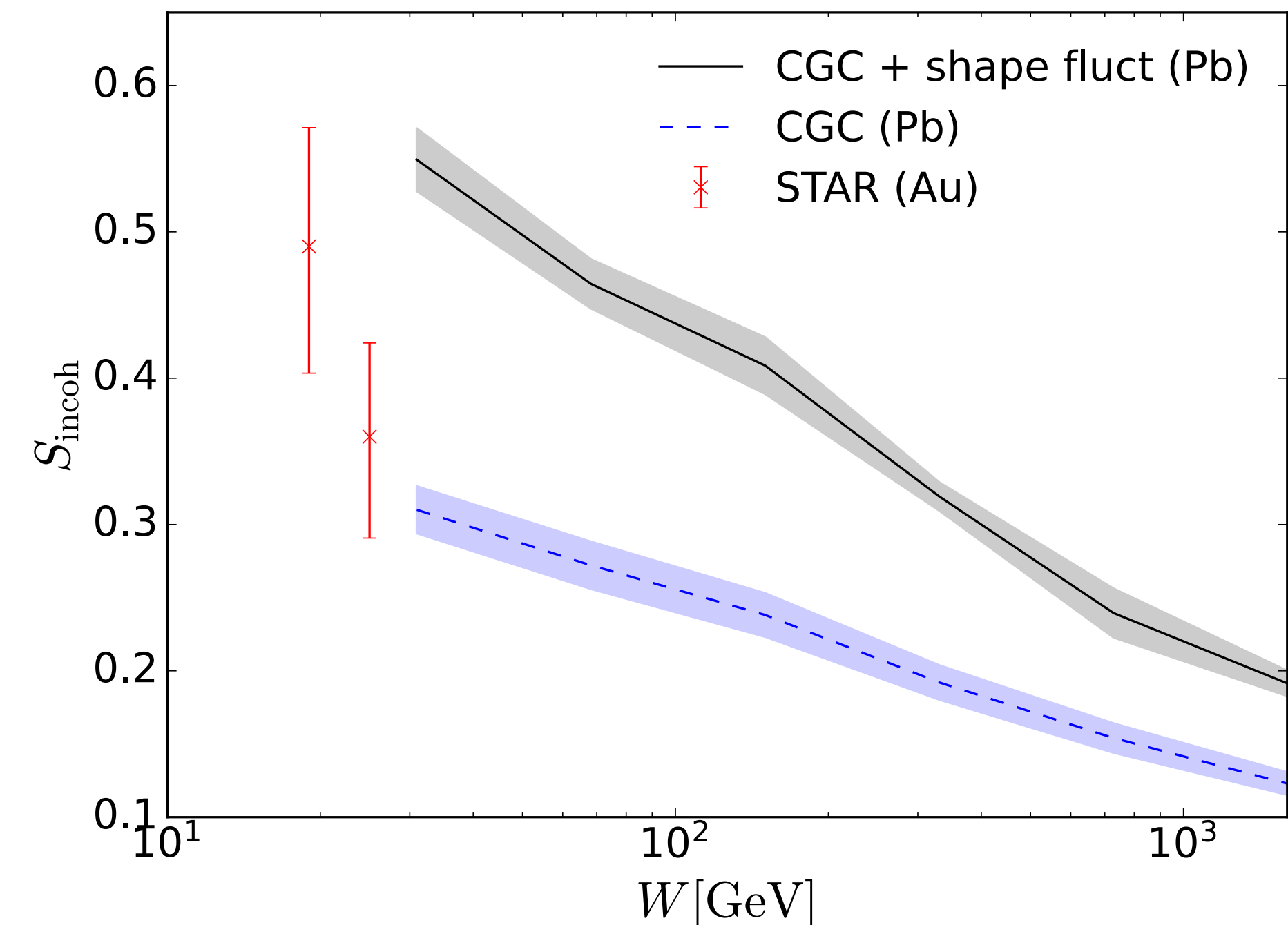
$$S_{\text{coh}} = \sqrt{\frac{\sigma^{\gamma A}}{\sigma^{\text{IA}}}} \quad \sigma^{\text{IA}} = \frac{d\sigma^{\gamma p}}{dt}(t=0) \int_{-t_{\text{min}}} dt |F(t)|^2$$

Coherent



$$S_{\text{incoh}} = \frac{\sigma^{\gamma+A \rightarrow J/\psi+A^*}}{A(\sigma^{\gamma+p \rightarrow J/\psi+p^*} + \sigma^{\gamma+p \rightarrow J/\psi+p})}$$

Incoherent



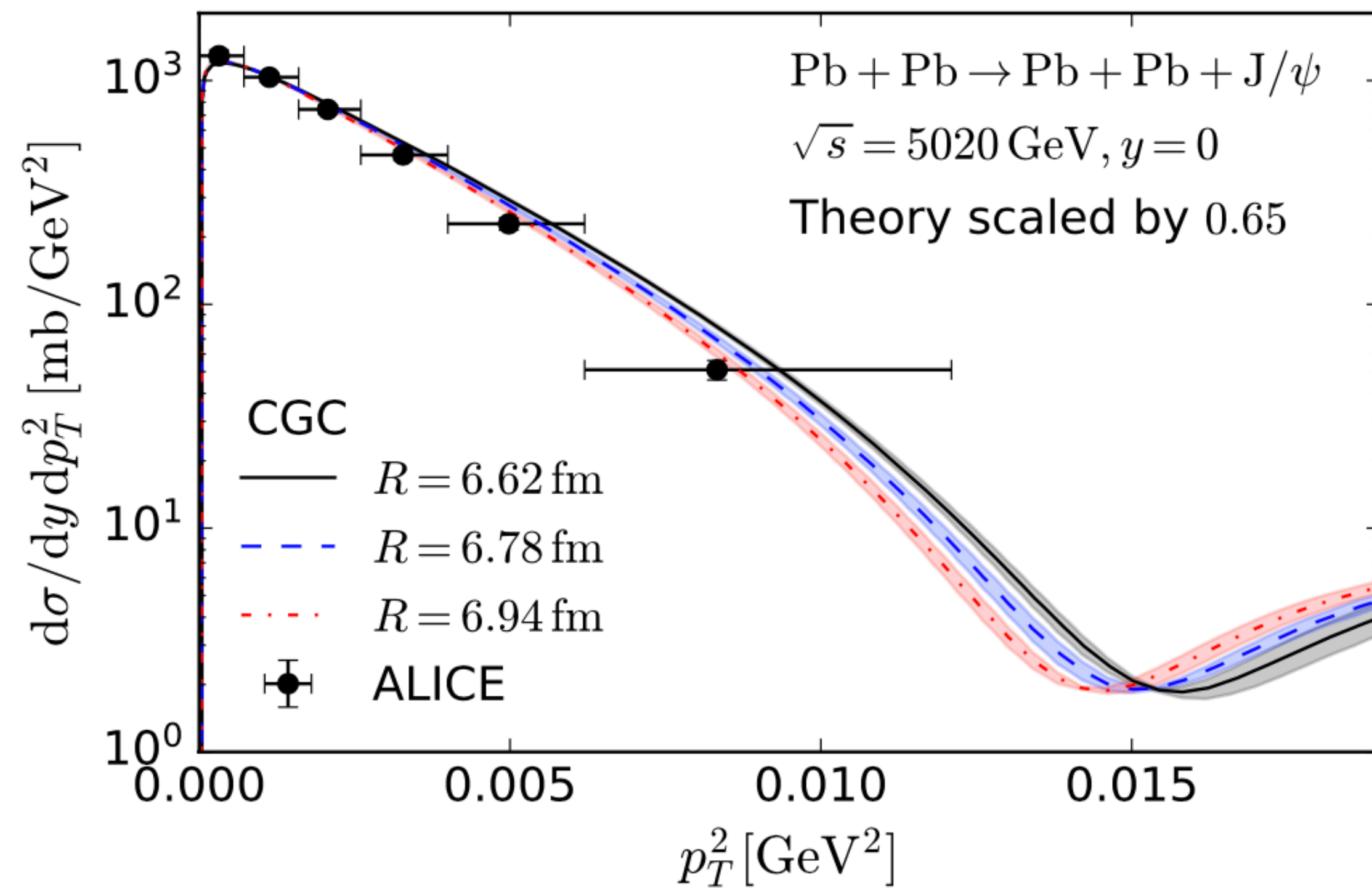
CMS Collaboration, A. Tumasyan et. al., Phys.Rev.Lett. 131 (2023) 26, 262301

ALICE Collaboration, S. Acharya et al, JHEP 10 119 (2023) [arXiv:2305:19060]

STAR Collaboration, Phys.Rev.Lett. 133 (2024) 5, 052301

Effect of the nuclear size

H. Mäntysaari, F. Salazar, B. Schenke, Phys.Rev.D 106 (2022) 7, 074019



- Steep enough spectrum obtained with a larger nucleus
- Neutron skin effect?

STAR measurements of diffractive photo production of ρ mesons and study of interference patterns in the angular distribution of $\rho^0 \rightarrow \pi^+\pi^-$ decays also indicate that strong-interaction nuclear radii of Au and U are larger than the charge radii
STAR Collaboration, Sci. Adv. 9, abq3903 (2023)

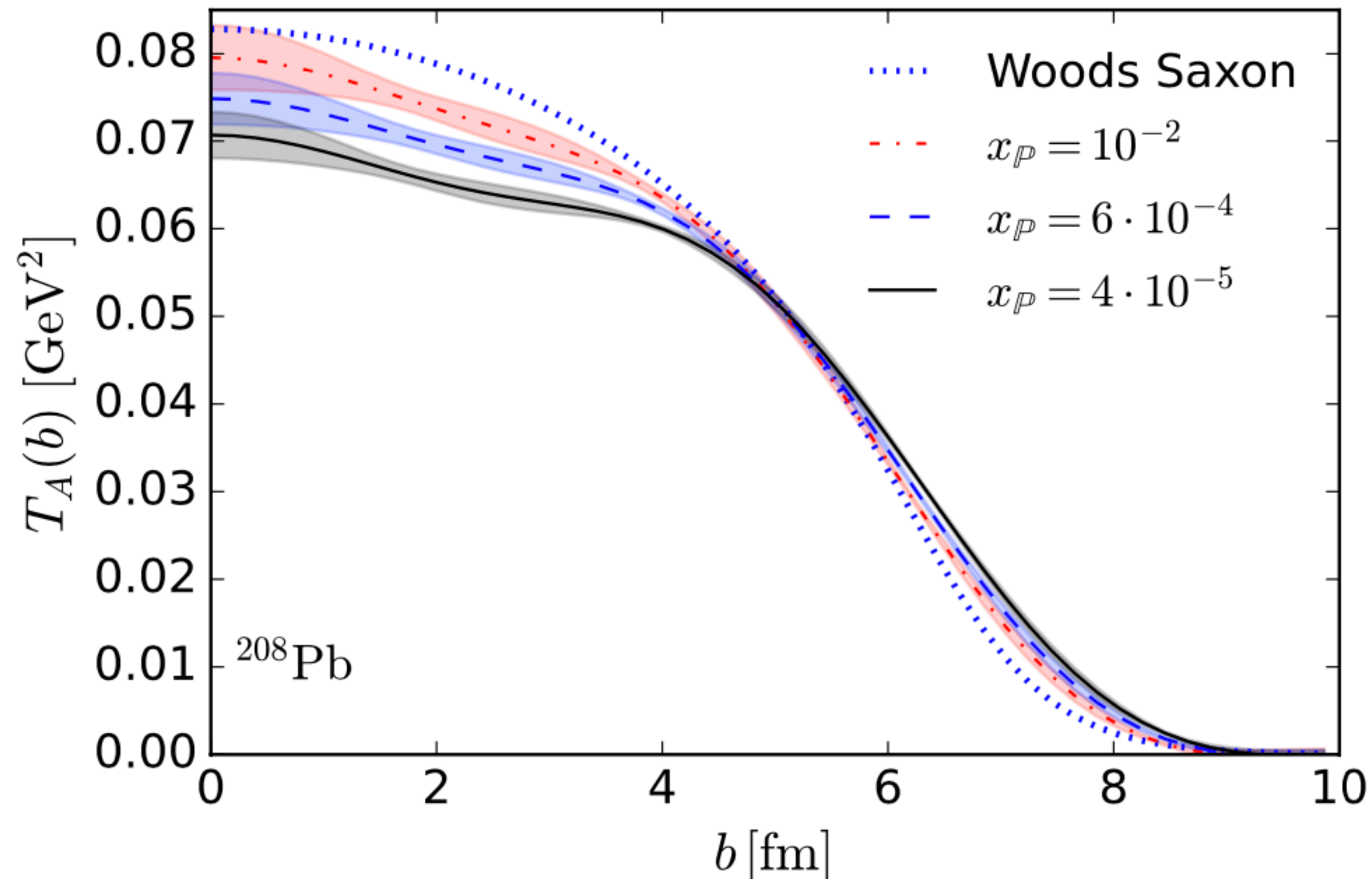
ALICE Collaboration, Phys.Lett.B 817 (2021) 136280

Saturation effects on nuclear geometry

H. Mäntysaari, F. Salazar, B. Schenke, Phys.Rev.D 106 (2022) 7, 074019

Fourier transform to coordinate space

$$T_A(b) \propto \int \Delta d\Delta J_0(b\Delta) (-1)^n \sqrt{\frac{d\sigma^{\gamma^* + \text{Pb} \rightarrow \text{J}/\psi + \text{Pb}}}{d|t|}},$$



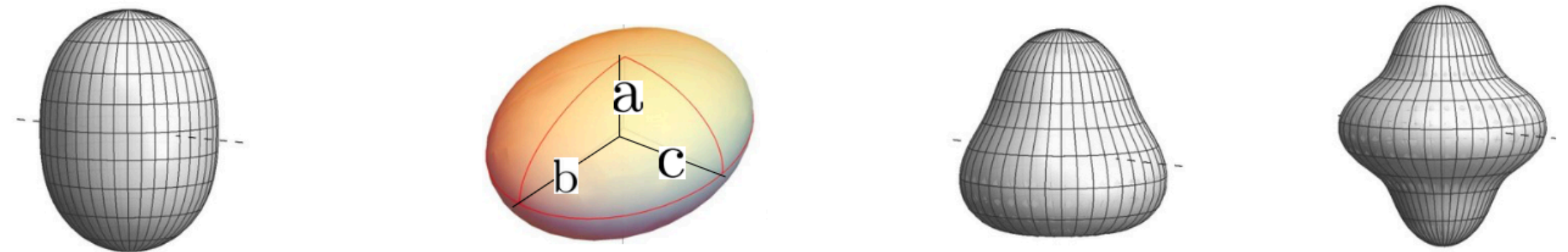
JIMWLK evolution leads to growth of the nucleus towards small x and depletion near the center (normalized so $\int d^2b T_A(b) = 208$)

Effects of deformation on diffractive cross sections

H. Mäntysaari, B. Schenke, C. Shen, W. Zhao, *Phys. Rev. Lett.* **131**, 062301 (2023)

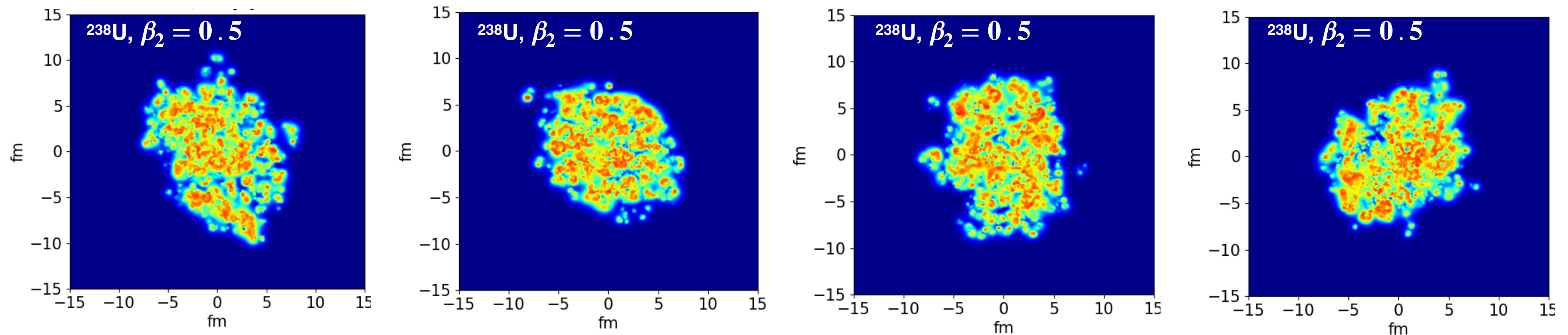
Implement deformation in the Woods-Saxon distribution:

$$\rho(r, \Theta, \Phi) \propto \frac{1}{1 + \exp([r - R(\Theta, \Phi)]/a)}, \quad R(\Theta, \Phi) = R_0 \left[1 + \beta_2 \left(\cos \gamma Y_{20}(\Theta) + \sin \gamma Y_{22}(\Theta, \Phi) \right) + \beta_3 Y_{30}(\Theta) + \beta_4 Y_{40}(\Theta) \right]$$



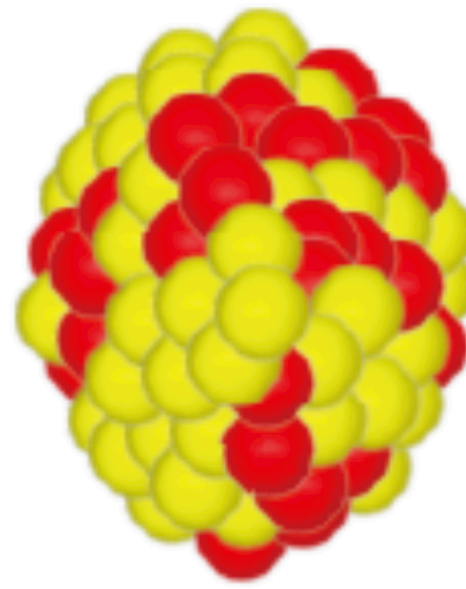
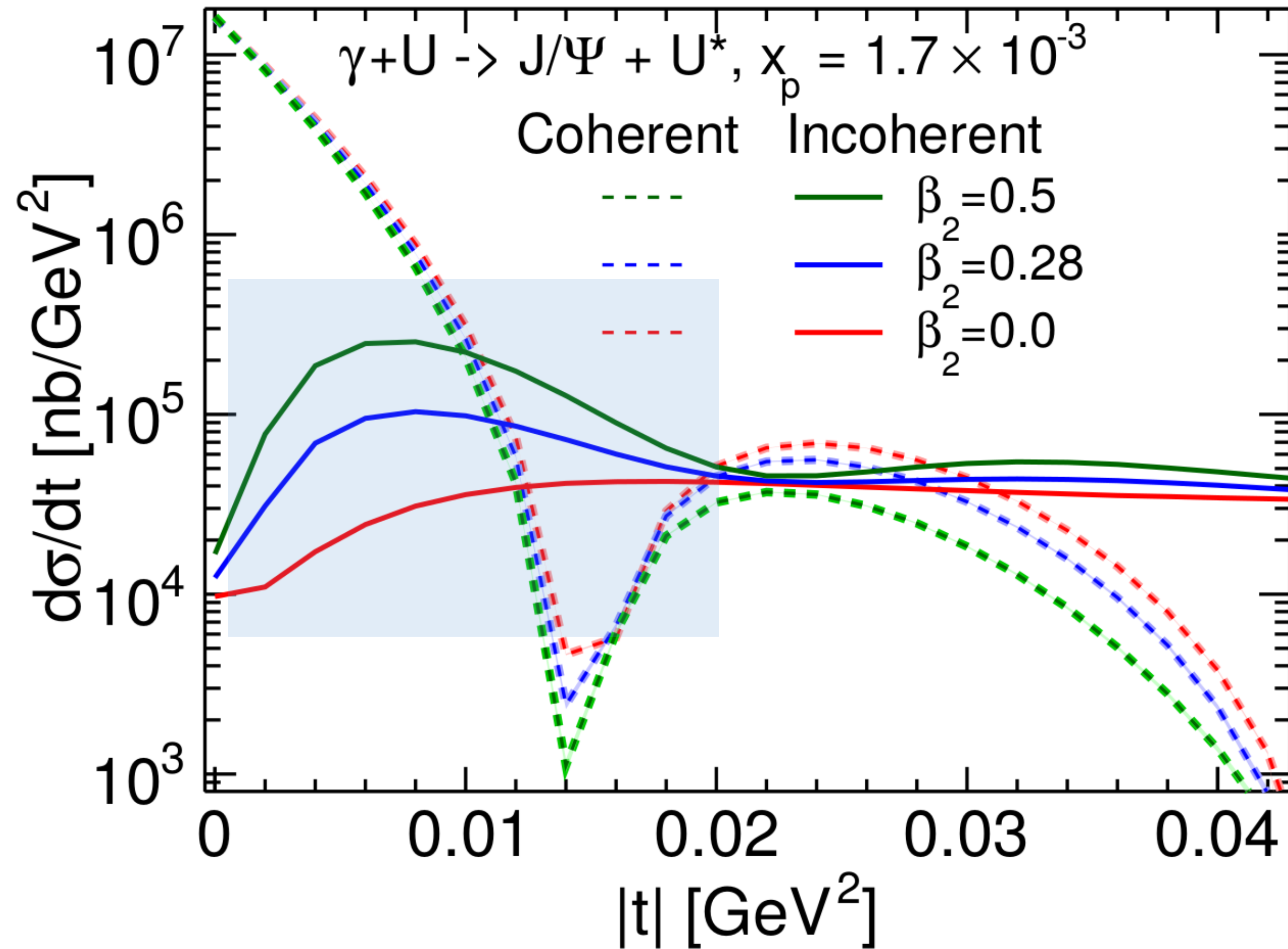
from G. Giacalone

Deformed nuclei exhibit larger fluctuation in the transverse projection:



Effects of deformation on diffractive cross sections

H. Mäntysaari, B. Schenke, C. Shen, W. Zhao, *Phys. Rev. Lett.* **131**, 062301 (2023)



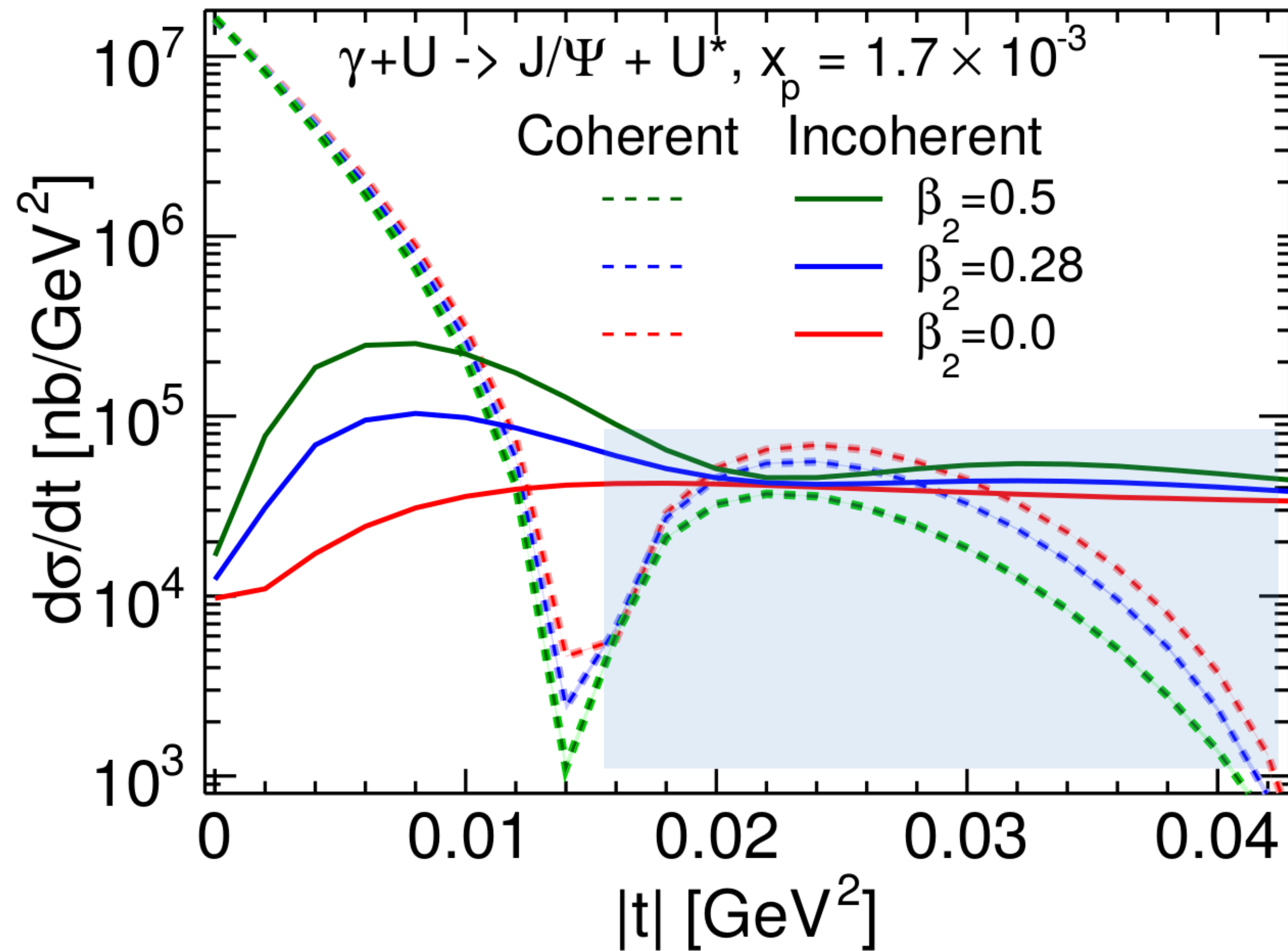
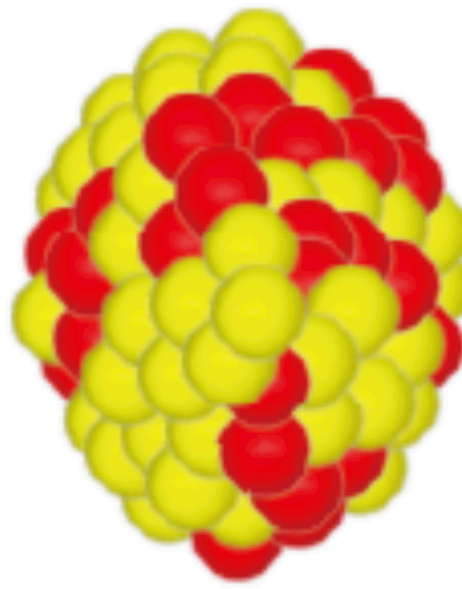
Deformation of the nucleus affects incoherent cross section at small $|t|$ (large length scales)

This observable provides direct information on the small x structure

$$Q^2 = 0$$

Effects of deformation on diffractive cross sections

H. Mäntysaari, B. Schenke, C. Shen, W. Zhao, *Phys. Rev. Lett.* **131**, 062301 (2023)



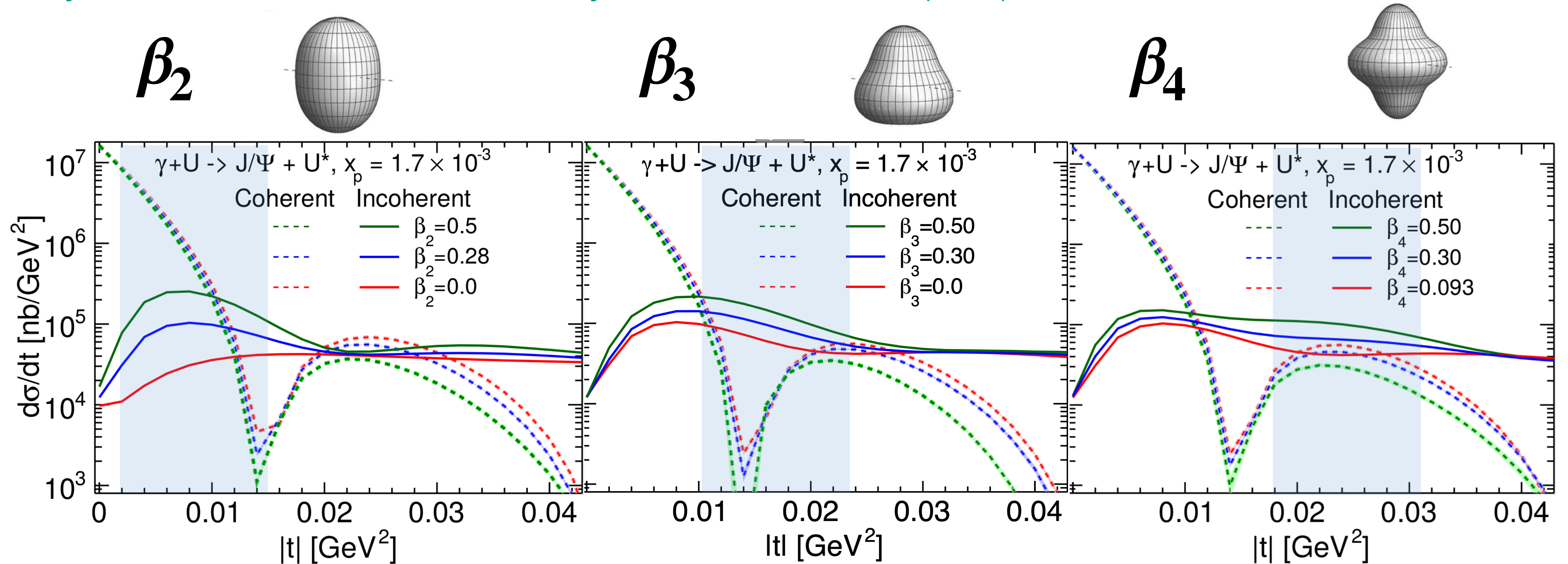
Deformation changes the shape of the average 2D projection of the nucleus



Modification of the coherent cross section

Effects of deformation on diffractive cross sections

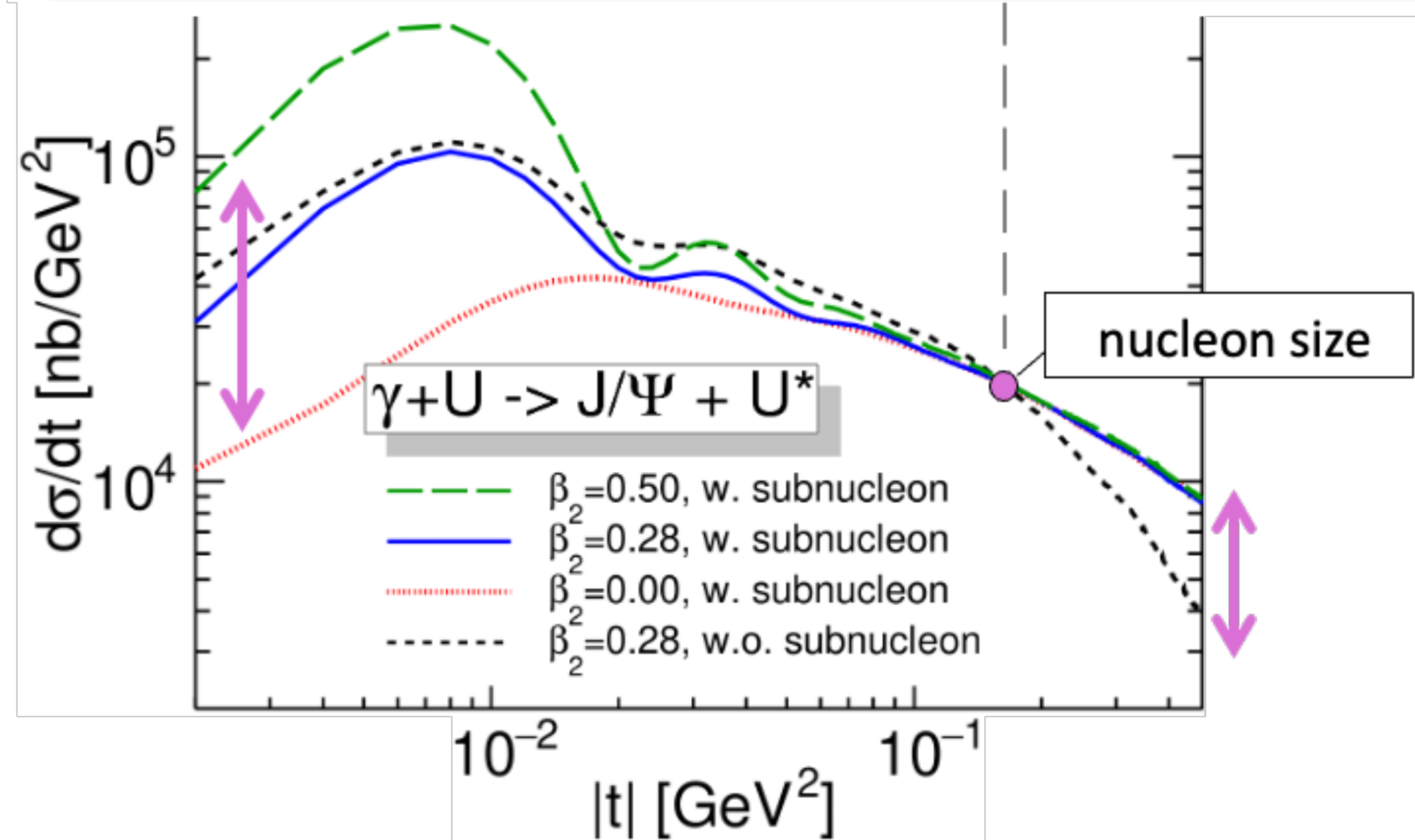
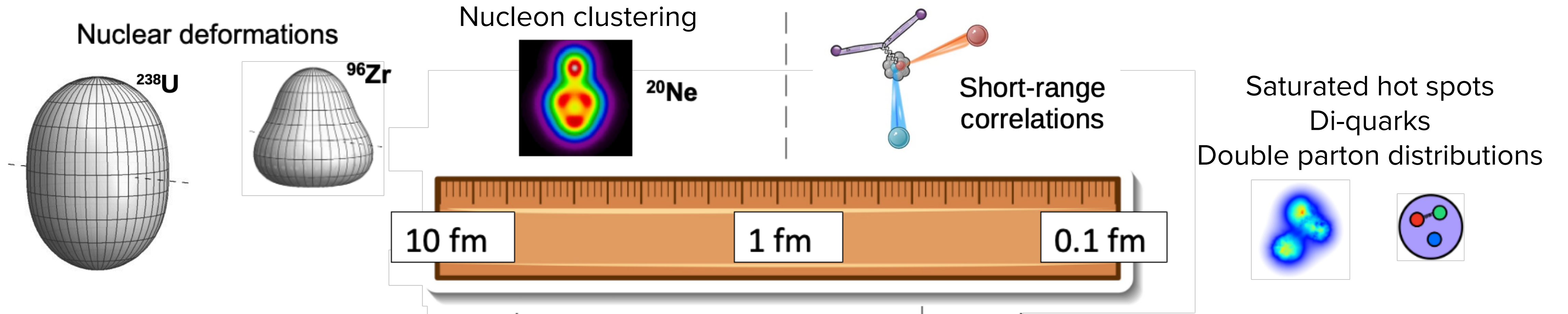
H. Mäntysaari, B. Schenke, C. Shen, W. Zhao, *Phys. Rev. Lett.* **131**, 062301 (2023)



- β_2 , β_3 and β_4 modify fluctuations at different length scales: Change incoherent cross section in different $|t|$ regions

Multi-scale sensitivity

H. Mäntysaari, B. Schenke, C. Shen, W. Zhao, Phys. Rev. Lett. 131, 062301 (2023)



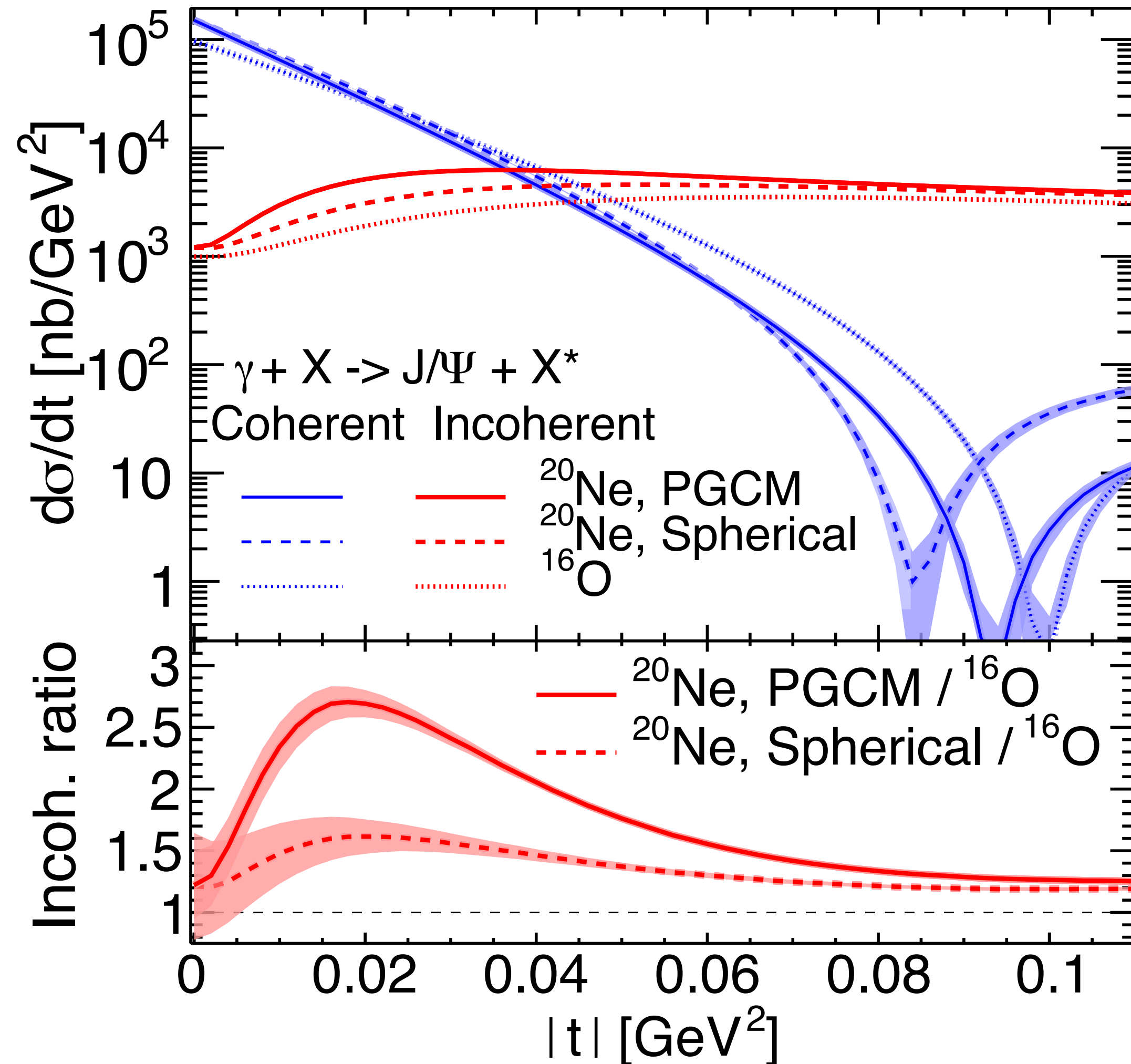
Chiral effective field theory
(low-energy QCD)



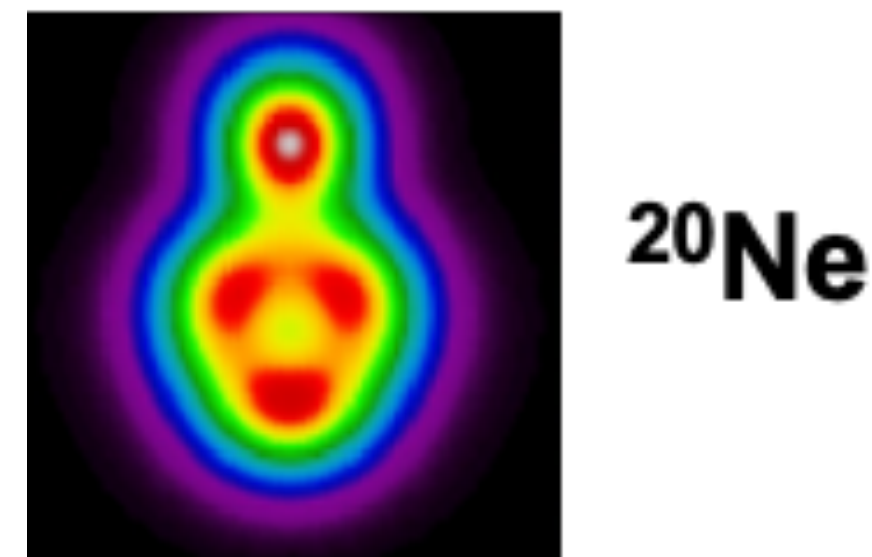
CGC effective field theory
(high-energy QCD)

Neon and Oxygen targets

H. Mäntysaari, B. Schenke, C. Shen, W. Zhao, *Phys. Rev. Lett.* **131**, 062301 (2023)



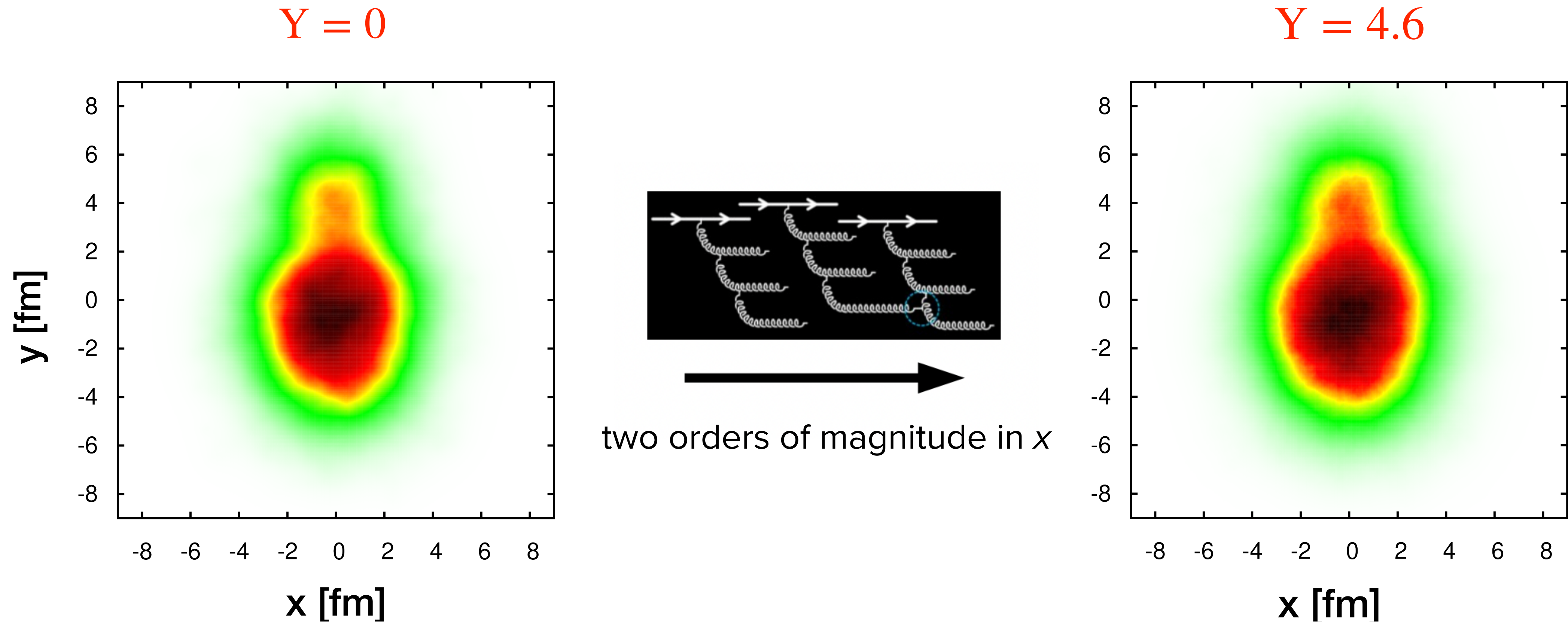
- ²⁰Ne has a bowling pin shape that leads to an increased incoherent cross section relative to an assumed spherical (on average) neon or a spherical oxygen



PGCM: Projected Generator Coordinate Method: B. Bally et al., “Deciphering small system collectivity with bowling-pin-shaped ²⁰Ne isotopes,” in preparation (2023); Mikael Frosini, Thomas Duguet, Jean-Paul Ebran, Benjamin Bally, Tobias Mongelli, Tomá’s R. Rodríguez, Robert Roth, and Vittorio Soma, *Eur. Phys. J. A* **58**, 63 (2022)

Neon - JIMWLK evolution

G. Giacalone, B. Schenke, S. Schlichting, P. Singh

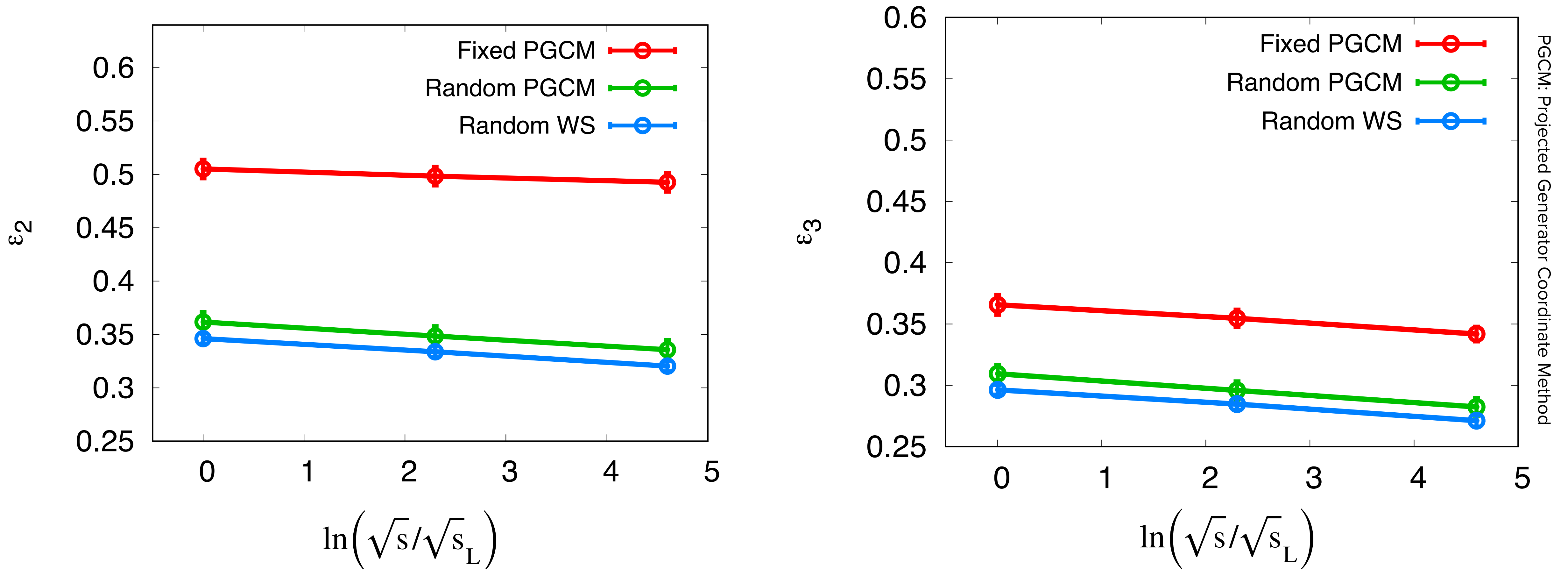


- Small- x evolution does not melt the bowling pin shape

Neon+Neon collisions - JIMWLK evolution

G. Giacalone, B. Schenke, S. Schlichting, P. Singh

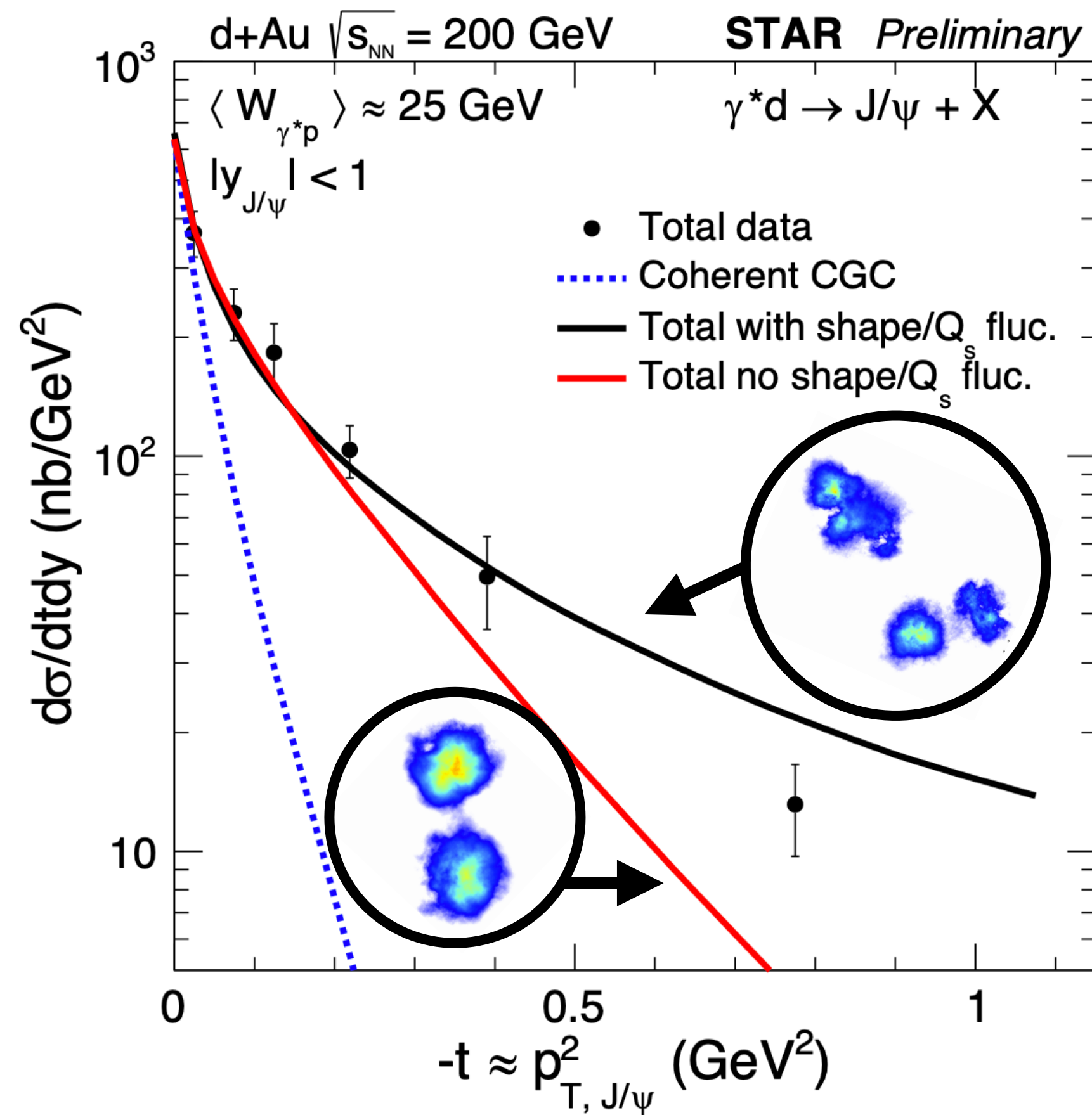
— After the collision at different energies (x), measure the spatial eccentricities



— Expected reduction - smoother distributions, but no large change

Photoproduction of J/ψ in d+Au collisions at STAR

H. Mäntysaari, B. Schenke, Phys. Rev. C101, 015203 (2020)



Substructure: large effect on incoherent at $|t| \gtrsim 0.25 \text{ GeV}^2$

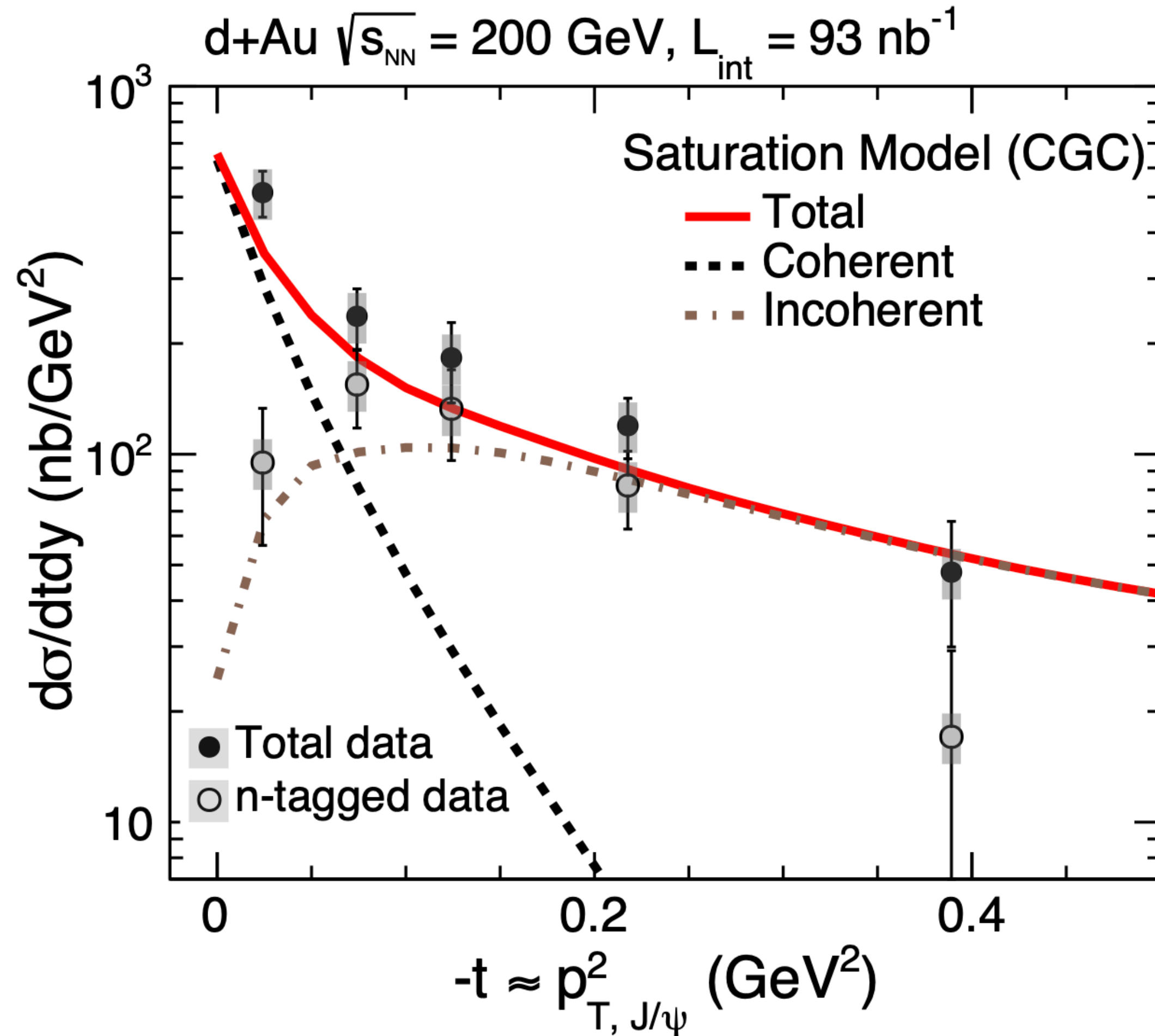
STAR data favors substructure

STAR Collaboration at Hard Probes 2020

PoS HardProbes2020 (2021) 100; arXiv:2009.04860

Photoproduction of J/ψ in d+Au collisions at STAR

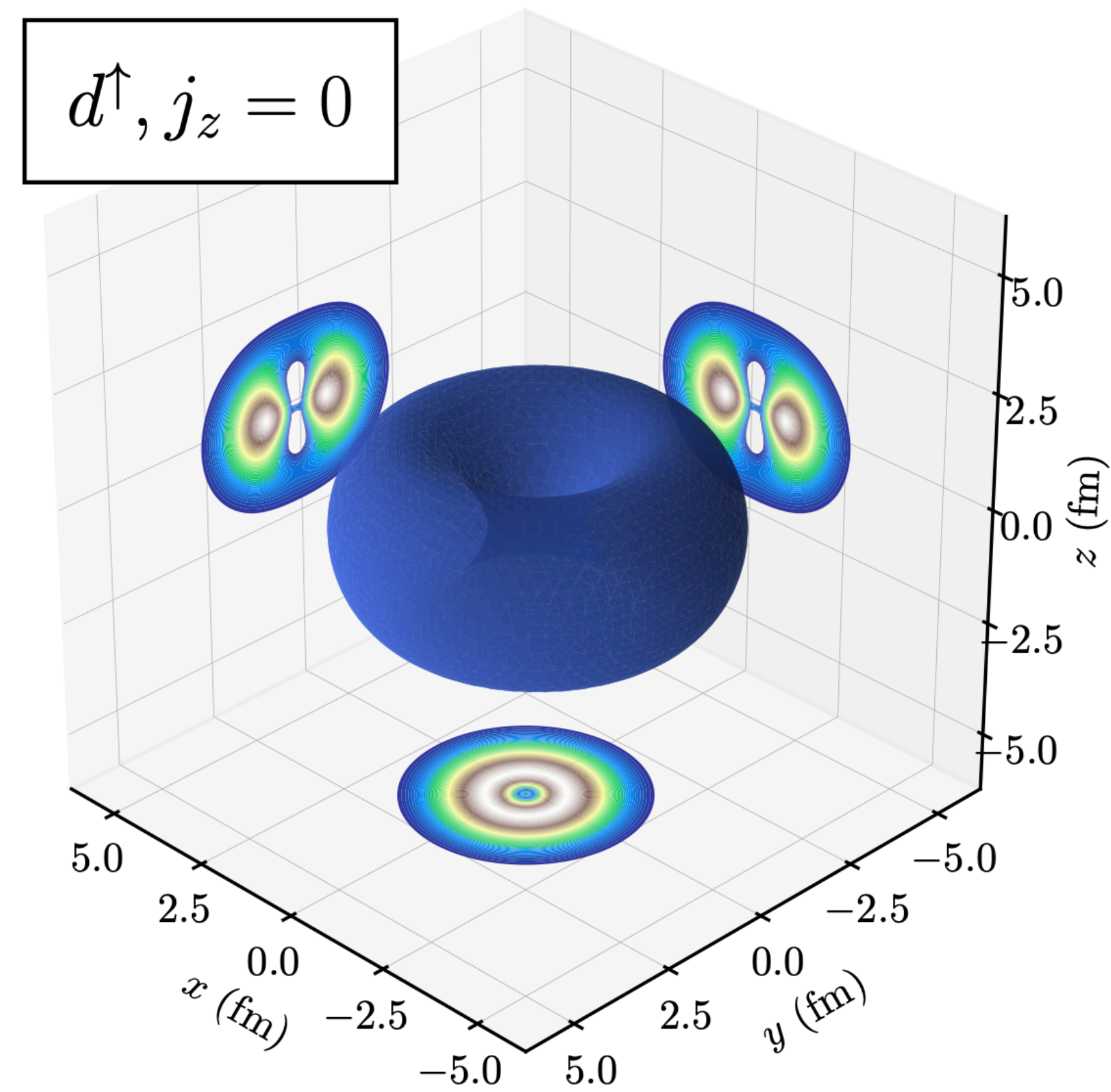
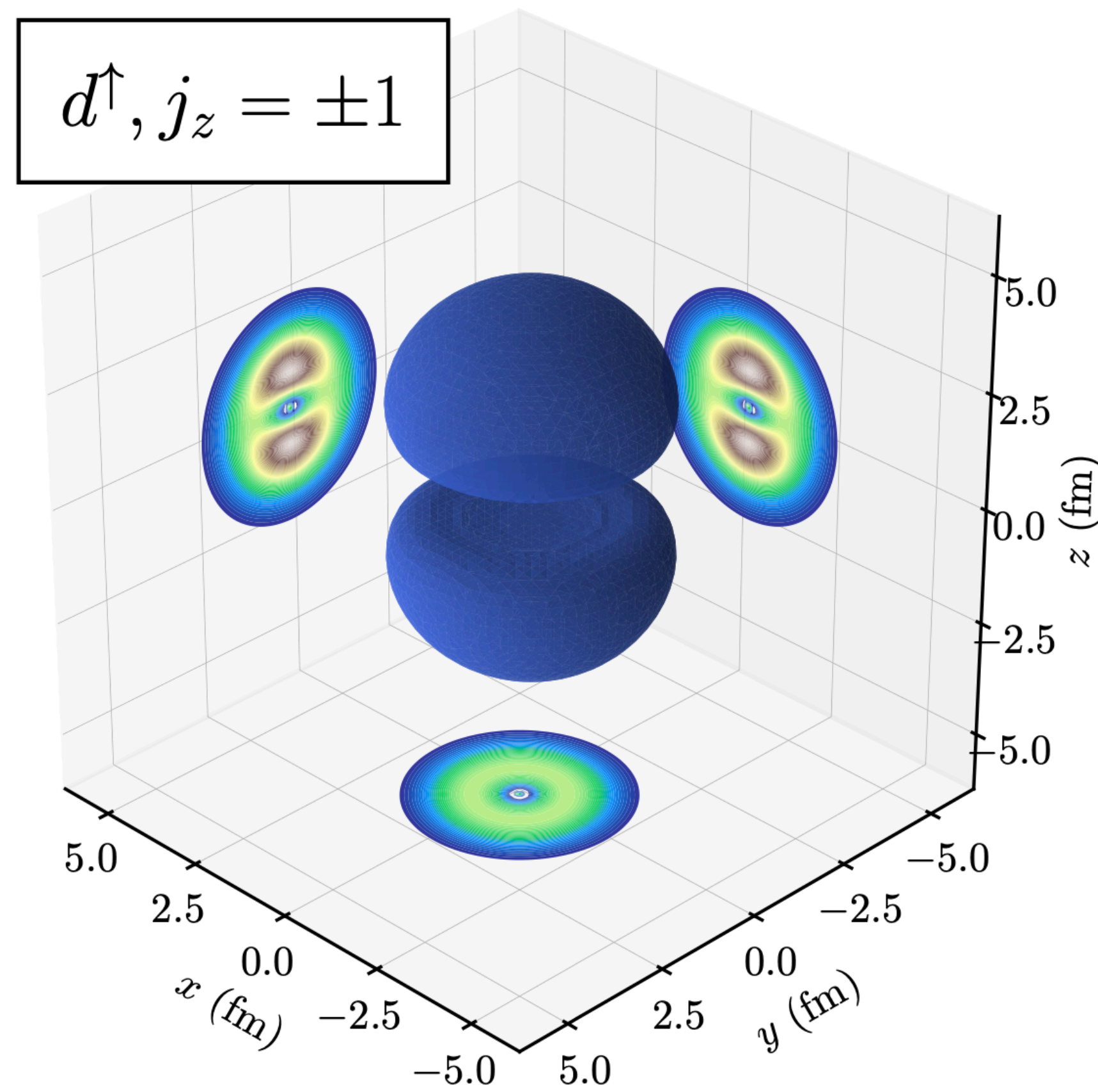
H. Mäntysaari, B. Schenke, *Phys. Rev. C*101, 015203 (2020)



n-tagged results can be compared to incoherent cross section

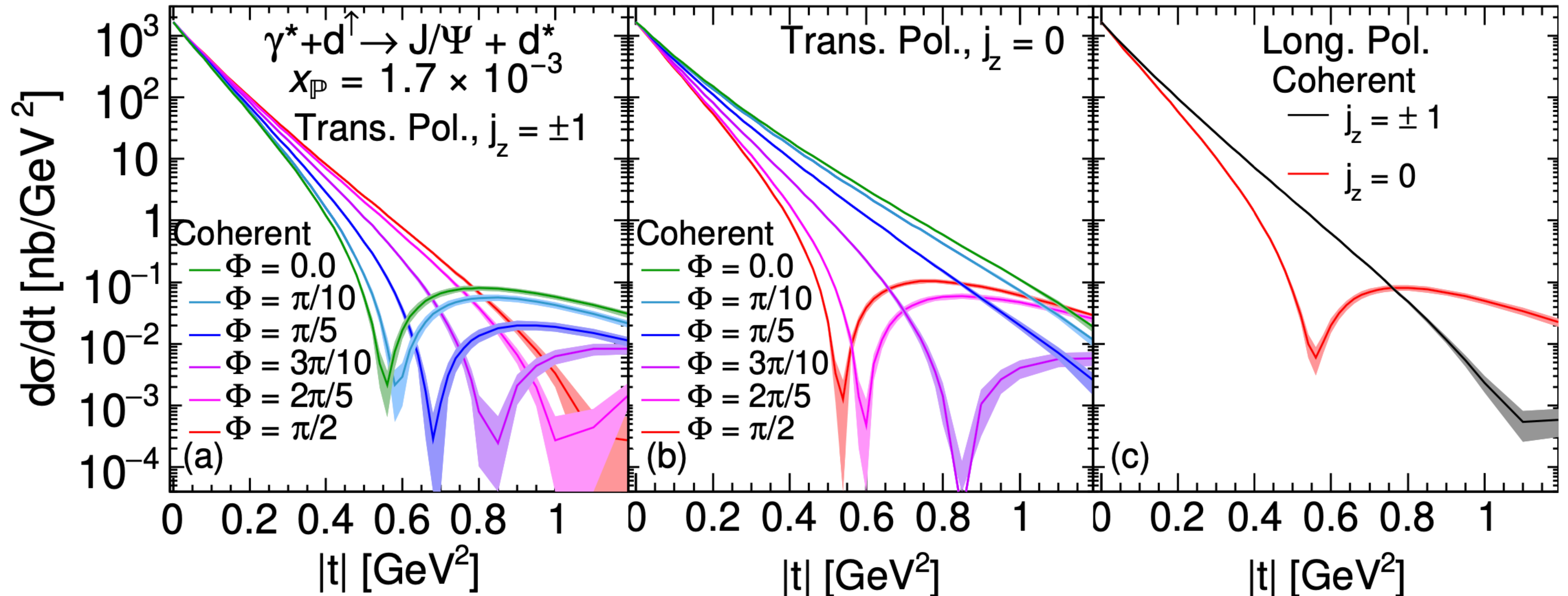
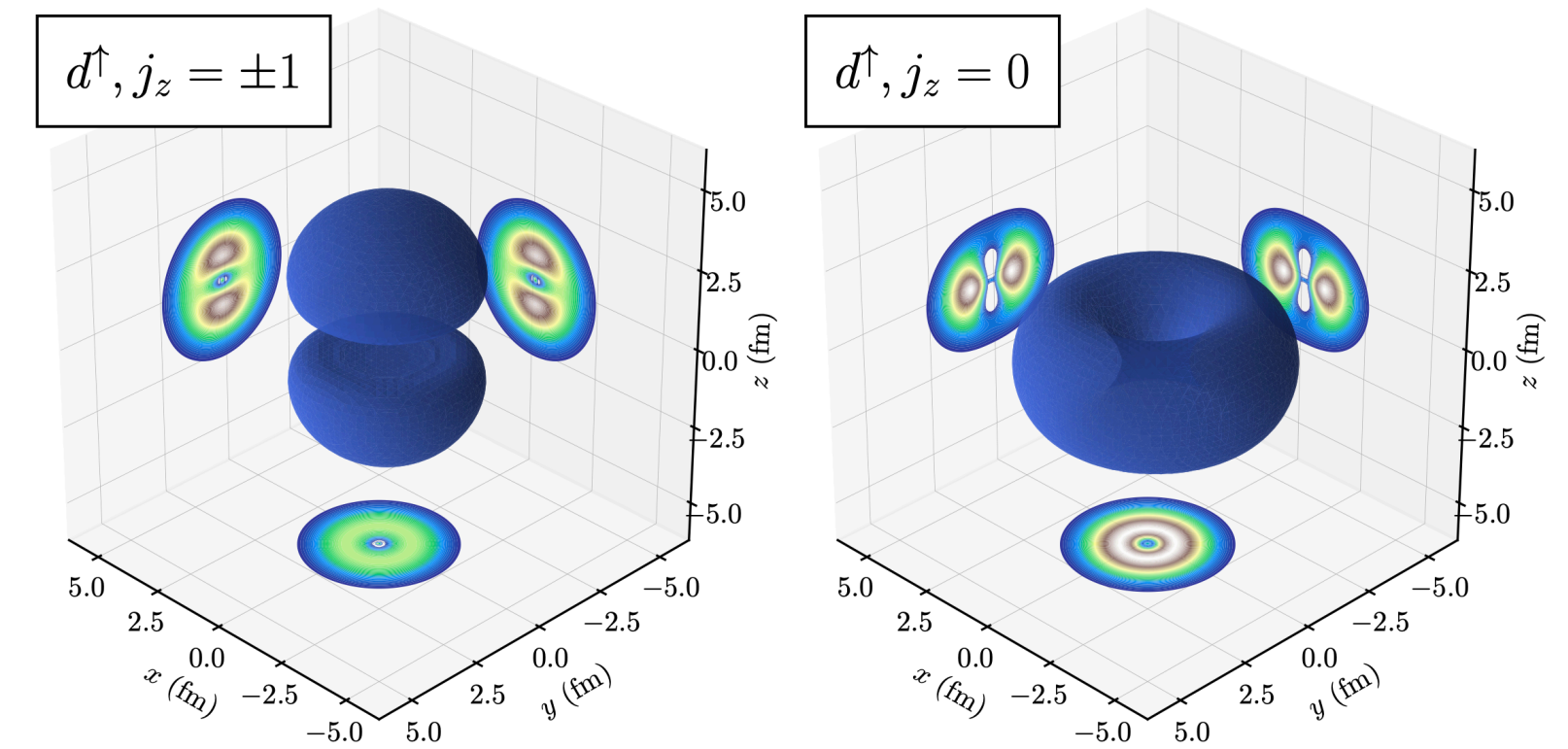
Polarized Deuteron

H. Mäntysaari, F. Salazar, B. Schenke, C. Shen, W. Zhao, Phys.Lett.B 858 (2024) 139053



Polarized Deuteron

H. Mäntysaari, F. Salazar, B. Schenke, C. Shen, W. Zhao
 Phys.Lett.B 858 (2024) 139053



Polarized Deuteron

H. Mäntysaari, F. Salazar, B. Schenke, C. Shen, W. Zhao, Phys.Lett.B 858 (2024) 139053

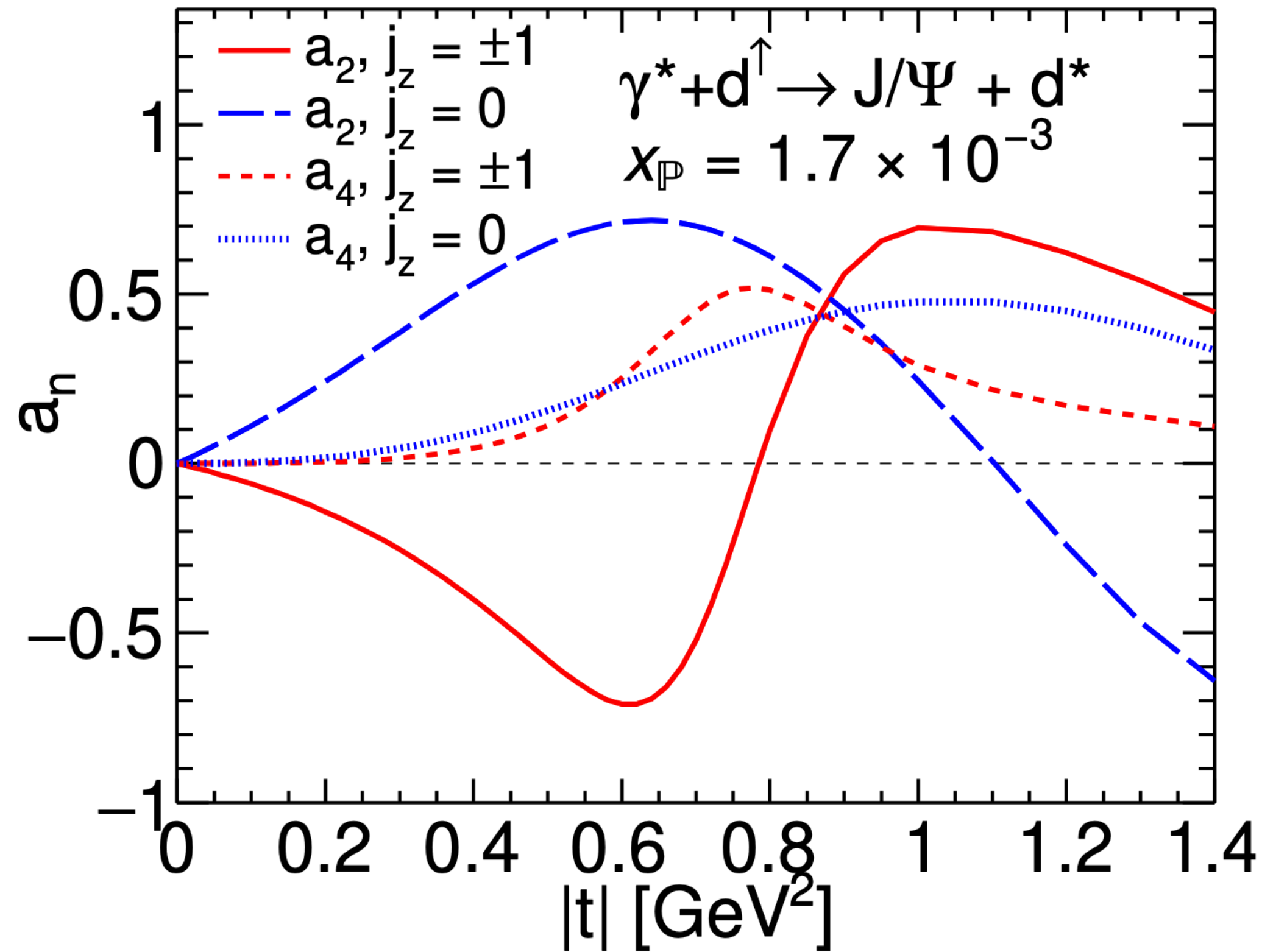


FIG. 4. Real parts of the second (a_2) and the fourth order (a_4) coefficients as functions of $|t|$ in transverse polarized $e + d$ collisions.

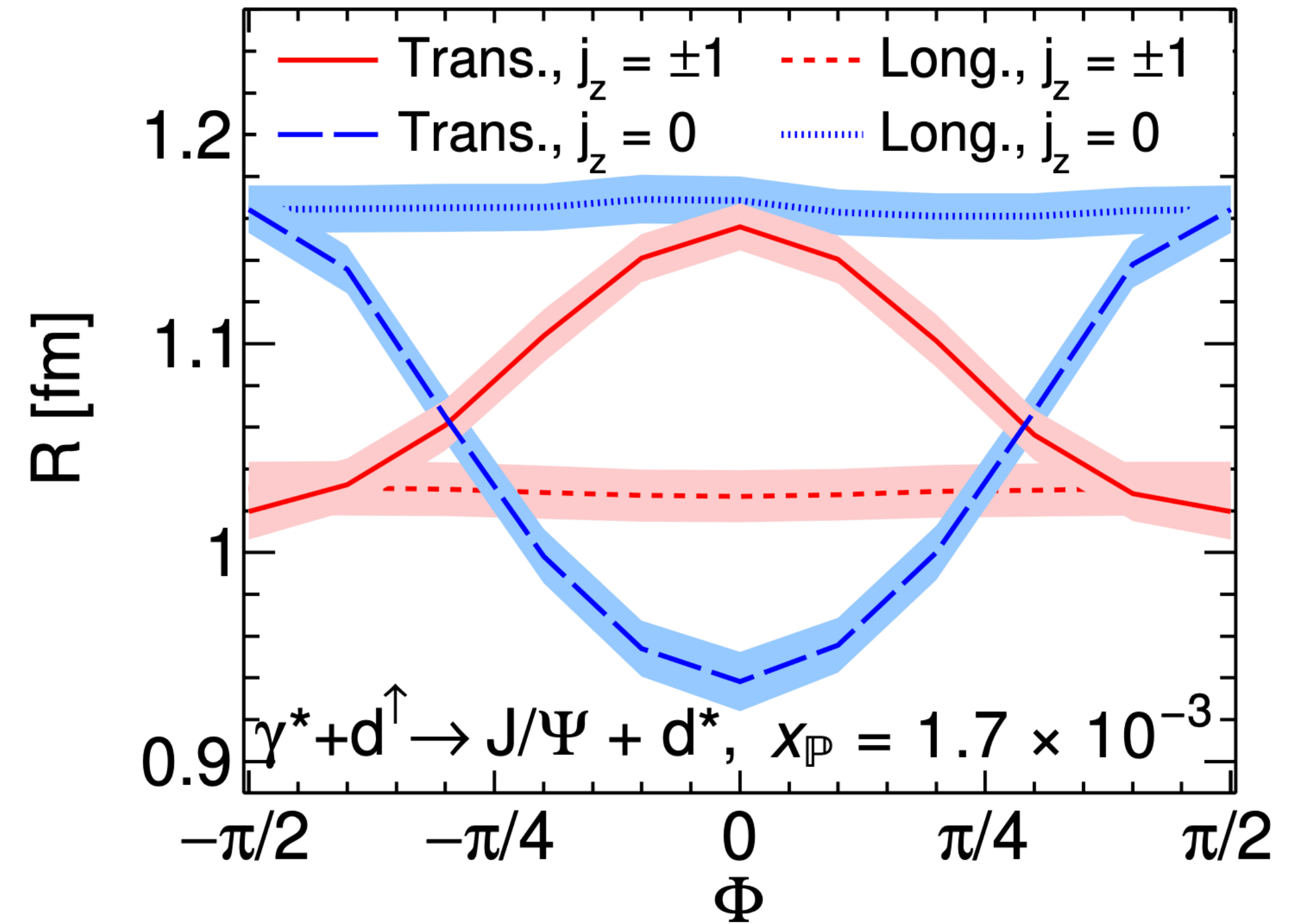
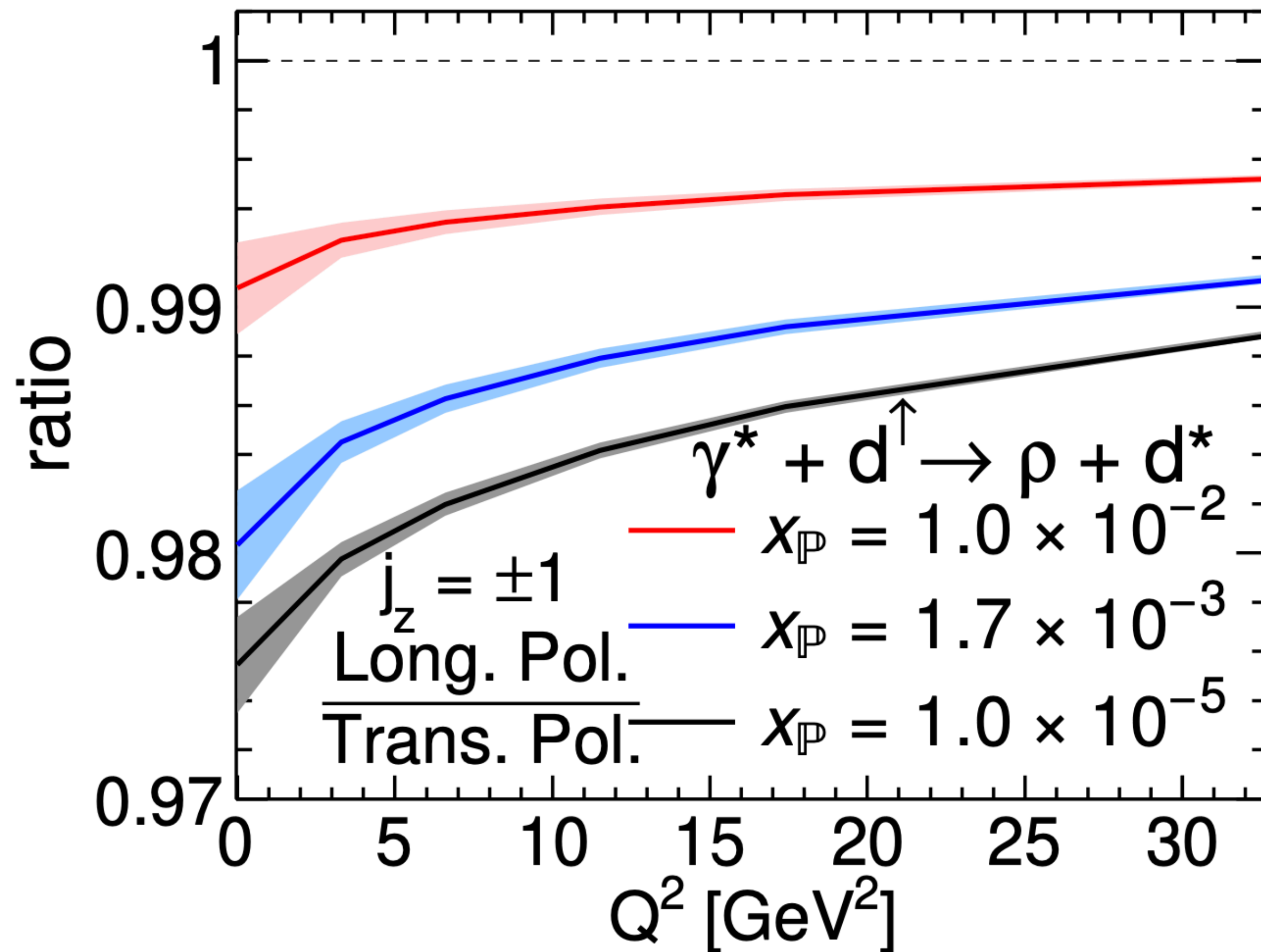


FIG. 5. The effective transverse radius as a function of the Φ angle defined relative to the polarization direction of transverse polarization.

Polarized Deuteron

H. Mäntysaari, F. Salazar, B. Schenke, C. Shen, W. Zhao, Phys.Lett.B 858 (2024) 139053



- Fixing the polarization allows to fix the orientation relative to the beam axis (for $Q^2=0$)
- This allows for testing saturation effects
- Small difference in coherent cross section at $t = 0$ for deuteron, as expected

Summary

- Diffractive vector meson production in UPCs:
Complementary way to access nuclear geometry
- Differential incoherent diffractive cross section sensitive to deformation at different length scales
- Difference between ^{20}Ne and ^{16}O up to factor of 2-3
- Deuteron data compatible with similar subnucleon fluctuations as observed in proton targets
- Polarized deuteron: Spatial structure of polarized wave function²

BACKUP

Interference effects

C. A. Bertulani, S. R. Klein and J. Nystrand, *Ann. Rev. Nucl. Part. Sci.* 55 (2005) 271

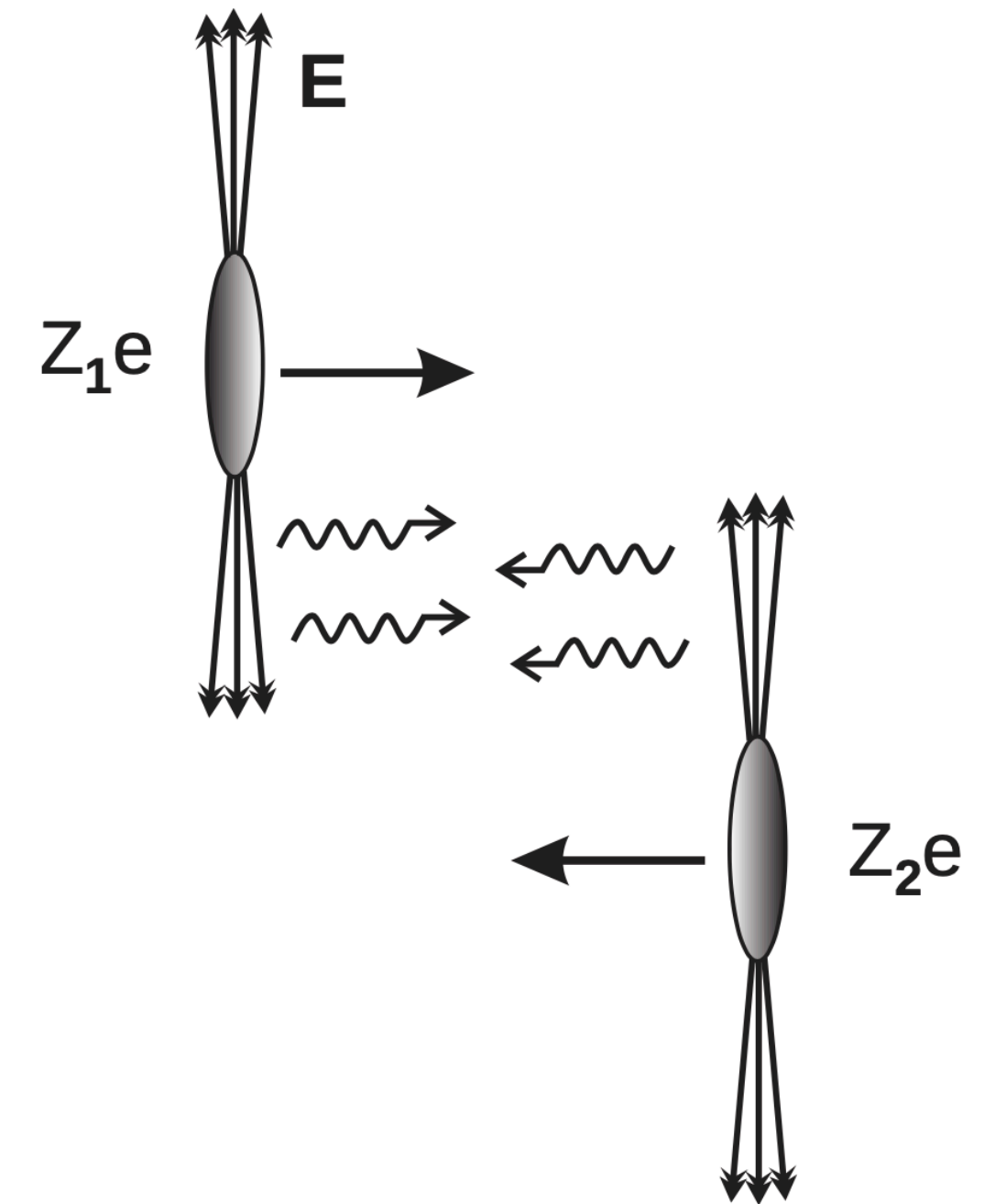
Interference is important for the differential cross-section in A+A, especially at midrapidity. There

$$\frac{d\sigma}{d|t|} = \frac{1}{16\pi} \int d^2\mathbf{B} |A_1 - A_2|^2 \theta(|\mathbf{B}| - 2R_A)$$

Interference is destructive in A+A because of negative parity of the VM

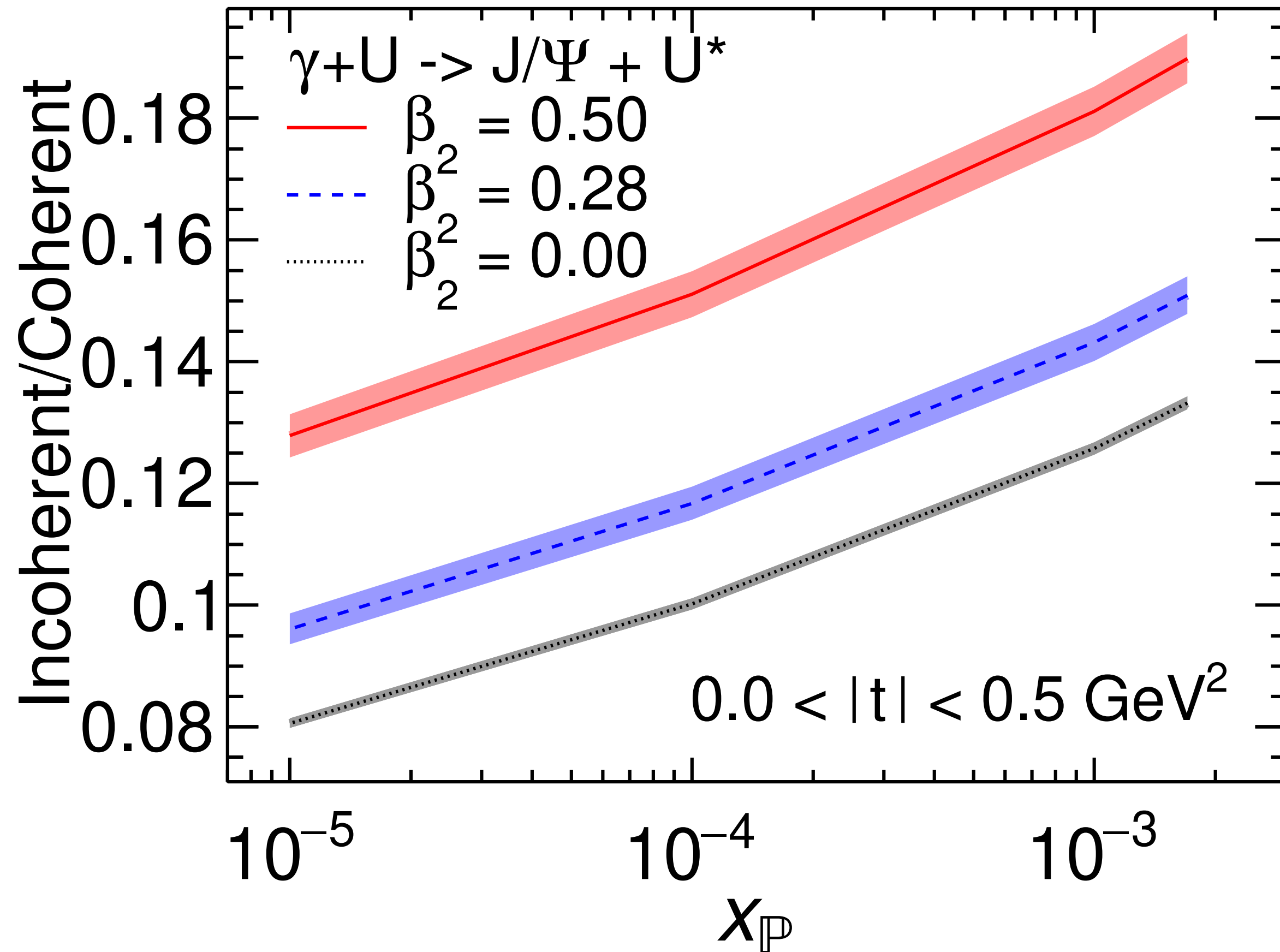
$$\left. \frac{d\sigma^{A_1+A_2 \rightarrow V+A_1+A_2}}{d|t| dy} \right|_{y=0} = 2 \int d^2\mathbf{B} n(\omega, |\mathbf{B}|) \frac{d\sigma^{\gamma+A \rightarrow V+A}}{d|t|} [1 - \cos(\mathbf{\Delta} \cdot \mathbf{B})] \theta(|\mathbf{B}| - 2R_A)$$

with $t = -\mathbf{\Delta}^2$



Towards smaller x

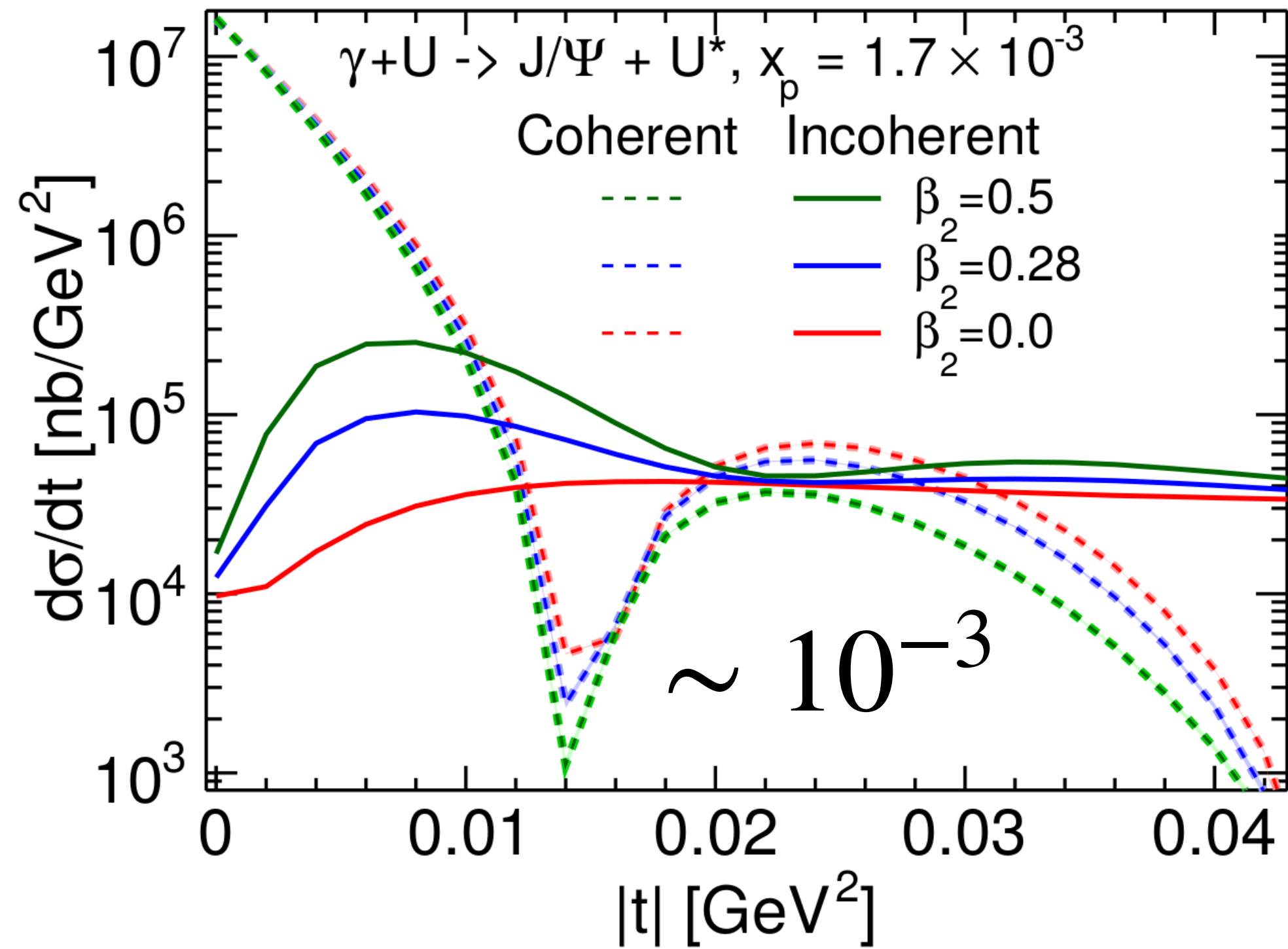
H. Mäntysaari, B. Schenke, C. Shen, W. Zhao, Phys. Rev. Lett. 131, 062301 (2023)



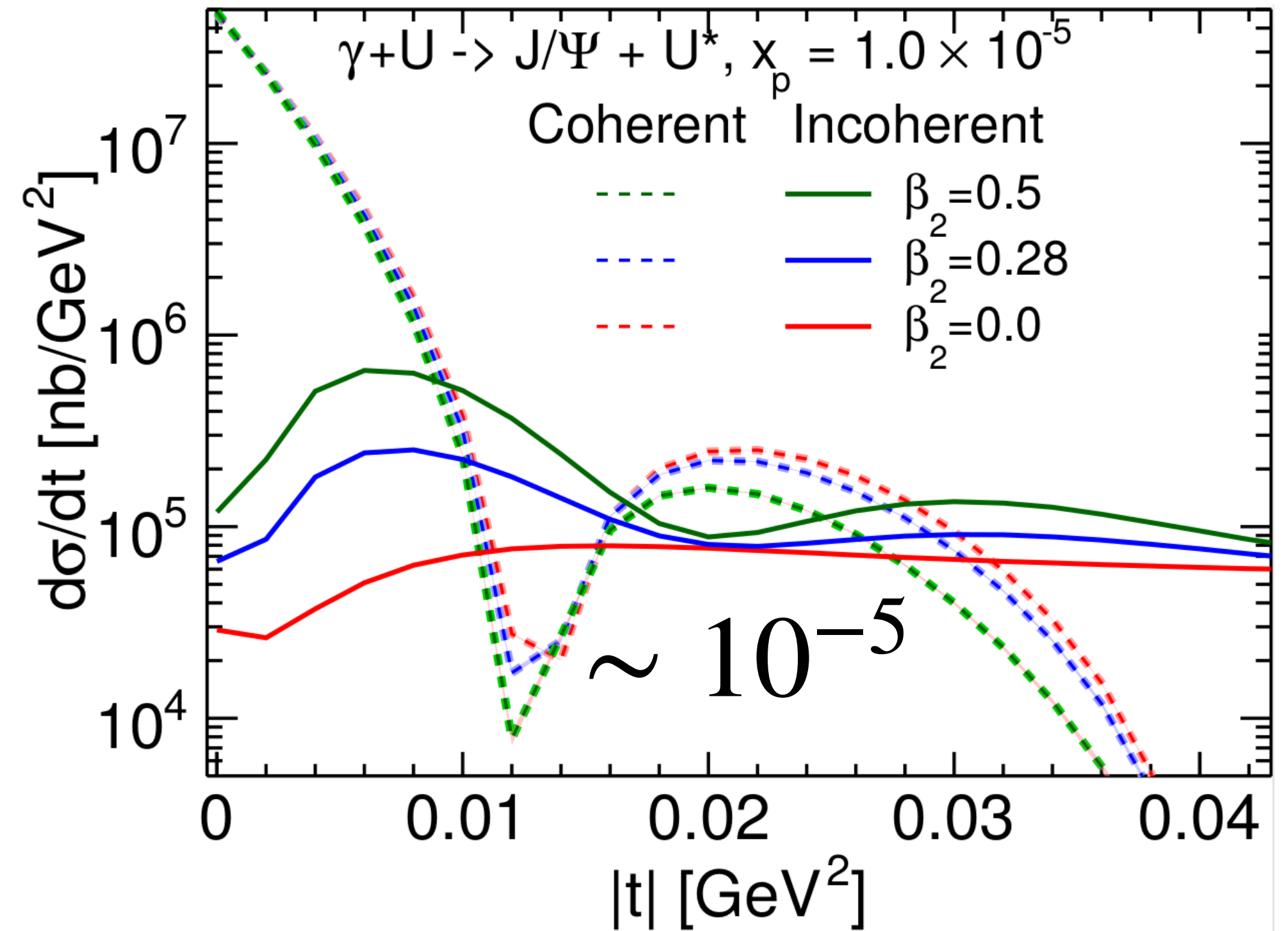
- JIMWLK evolution to smaller x
- Both cross sections increase
- Ratio incoherent/coherent decreases because fluctuations are reduced (nucleus becomes smoother)
- Difference between different β_2 does not decrease noticeably in this x range
- Is there a large enough x range we can cover at the EIC (at least $10^{-3} - 10^{-2}$)?

Towards smaller x : Do deformation effects survive?

H. Mäntysaari, B. Schenke, C. Shen, W. Zhao, in progress



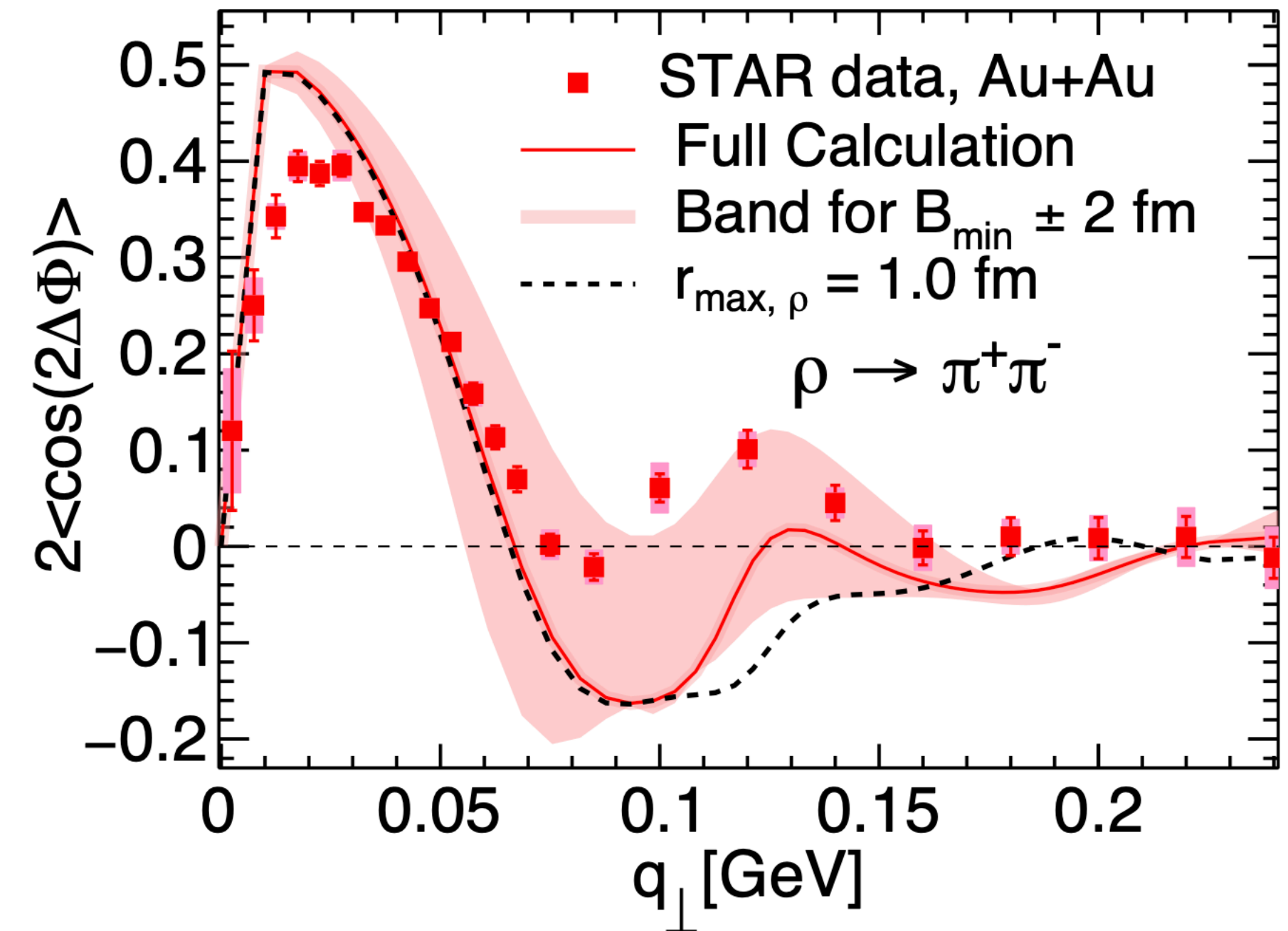
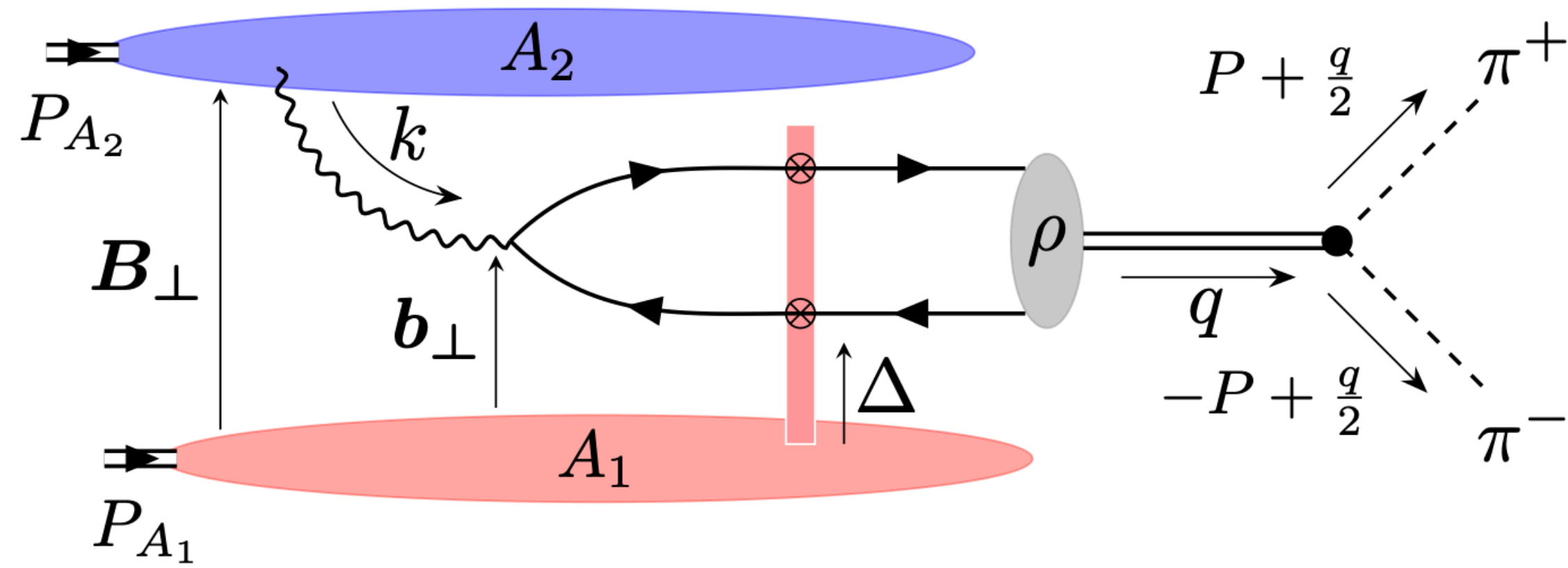
JIMWLK



Some changes in the cross section, but deformation effects survive

Angular anisotropies: Interference effects - ρ production

Heikki Mäntysaari, Farid Salazar, Björn Schenke, Chun Shen, Wenbin Zhao, arXiv:2310.15300



$$\frac{d\sigma^{\rho \rightarrow \pi^+ \pi^-} (\phi \rightarrow K^+ K^-)}{d^2\mathbf{P}_\perp d^2\mathbf{q}_\perp dy_1 dy_2} = \frac{1}{4(2\pi)^3} \frac{P_\perp^2 f^2}{(Q^2 - M_V^2)^2 + M_V^2 \Gamma^2} \left\{ C_0(x_1, x_2, |\mathbf{q}_\perp|) + C_2(x_1, x_2, |\mathbf{q}_\perp|) \cos(2(\phi_{\mathbf{P}_\perp} - \phi_{\mathbf{q}_\perp})) \right\}$$

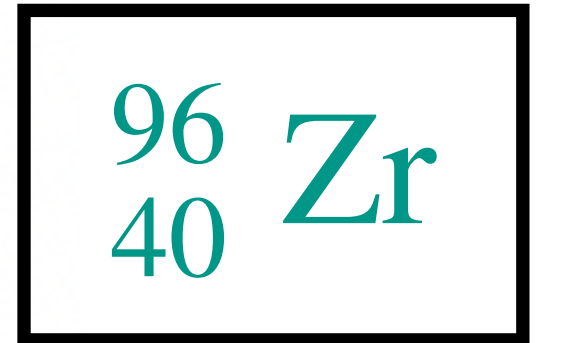
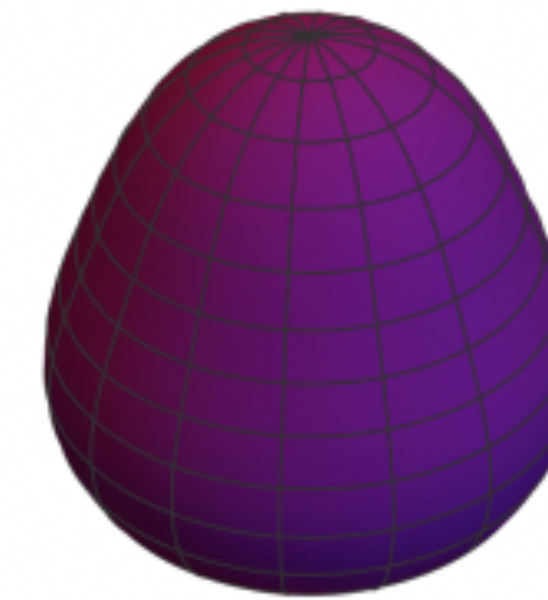
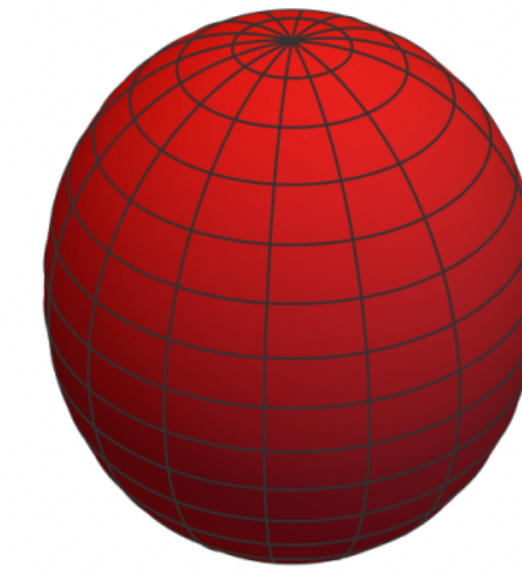
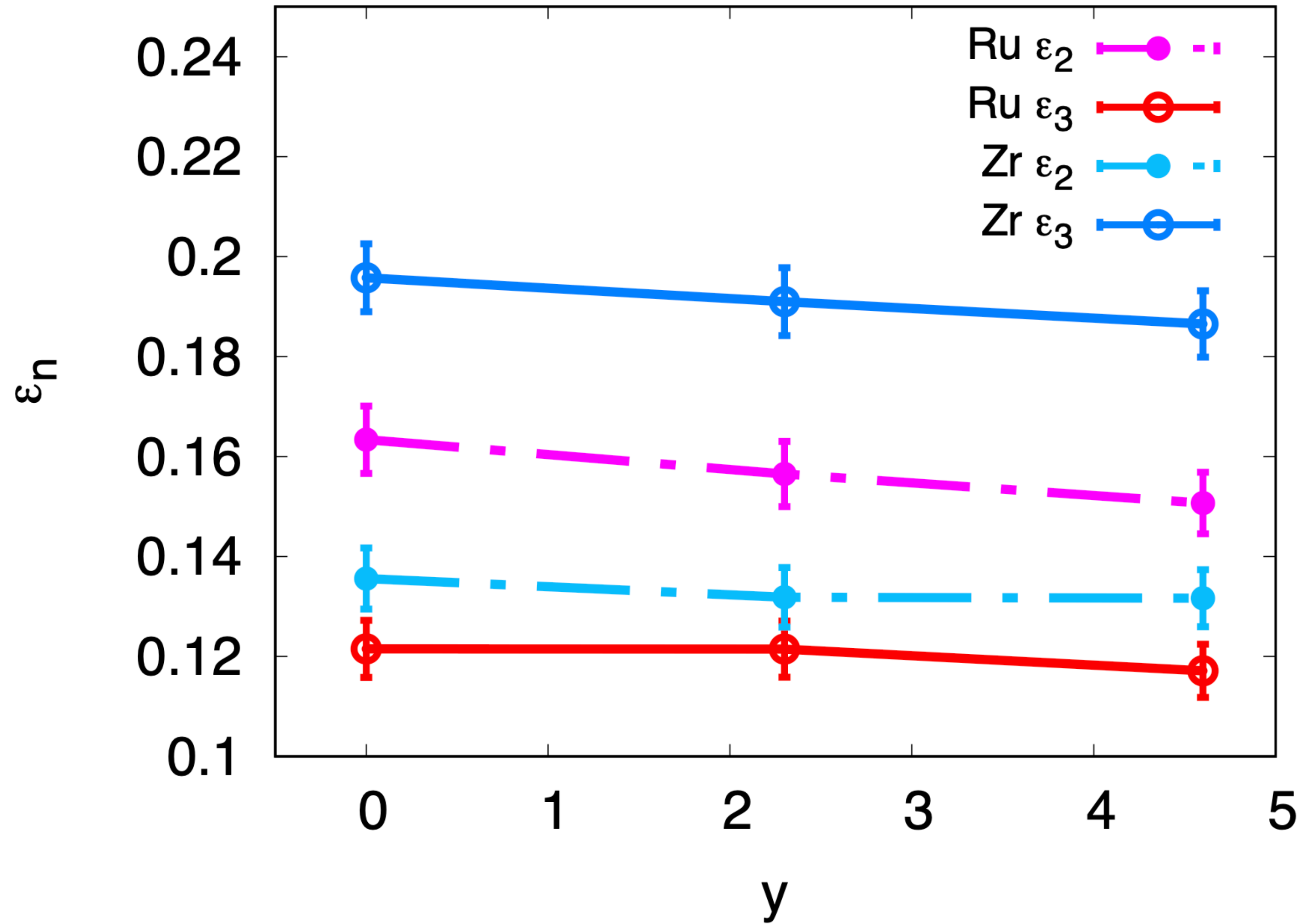
where

$$C_0(x_1, x_2, |\mathbf{q}_\perp|) = \left\langle \int d^2\mathbf{B}_\perp \mathcal{M}^i(x_1, x_2, \mathbf{q}_\perp, \mathbf{B}_\perp) \mathcal{M}^{\dagger,i}(x_1, x_2, \mathbf{q}_\perp, \mathbf{B}_\perp) \Theta(|\mathbf{B}_\perp| - B_{\min}) \right\rangle_\Omega, \text{ and}$$

$$C_2(x_1, x_2, |\mathbf{q}_\perp|) = \left(\frac{2\mathbf{q}_\perp^i \mathbf{q}_\perp^j}{q_\perp^2} - \delta^{ij} \right) \left\langle \int d^2\mathbf{B}_\perp \mathcal{M}^i(x_1, x_2, \mathbf{q}_\perp, \mathbf{B}_\perp) \mathcal{M}^{\dagger,j}(x_1, x_2, \mathbf{q}_\perp, \mathbf{B}_\perp) \Theta(|\mathbf{B}_\perp| - B_{\min}) \right\rangle_\Omega$$

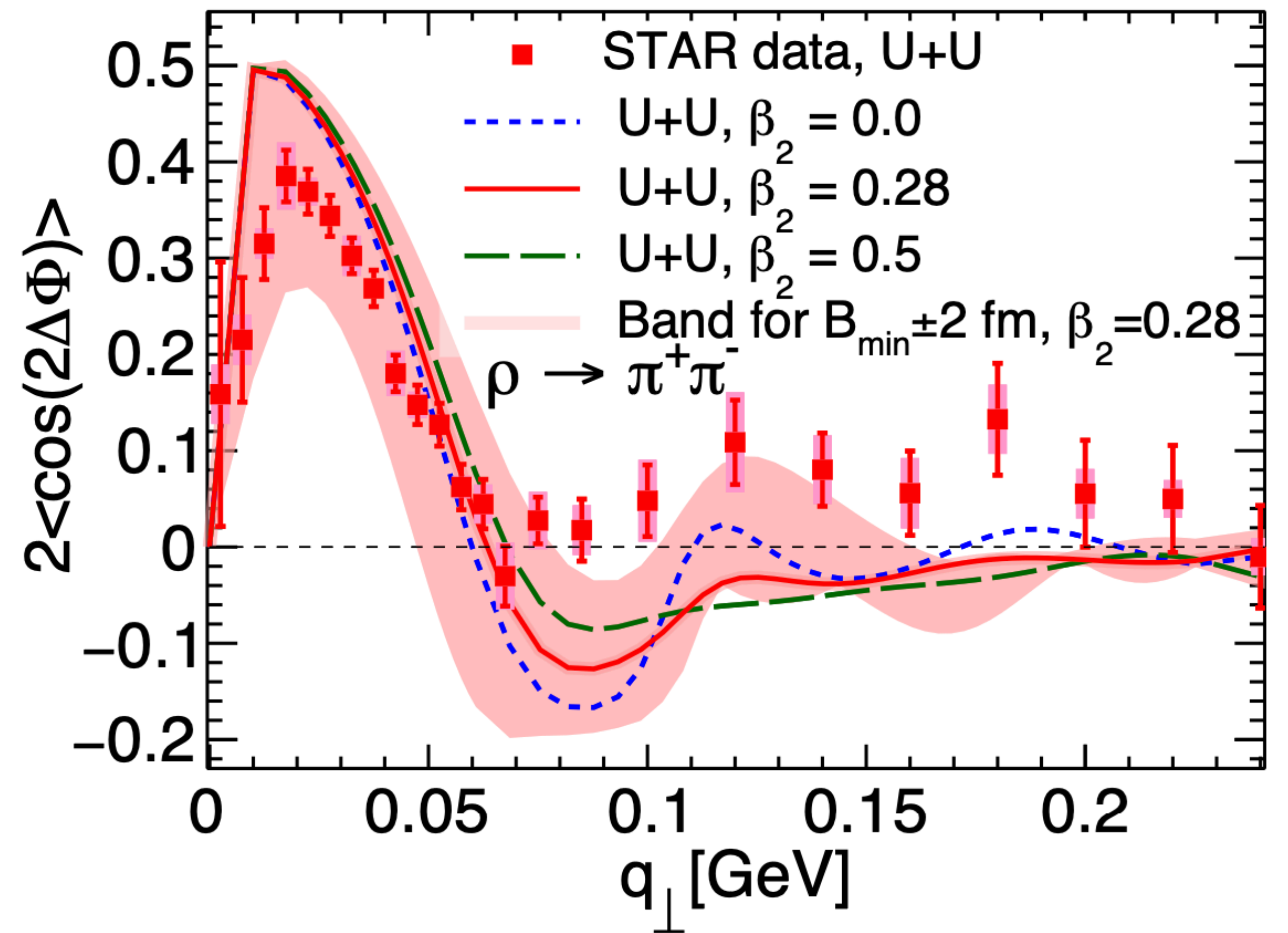
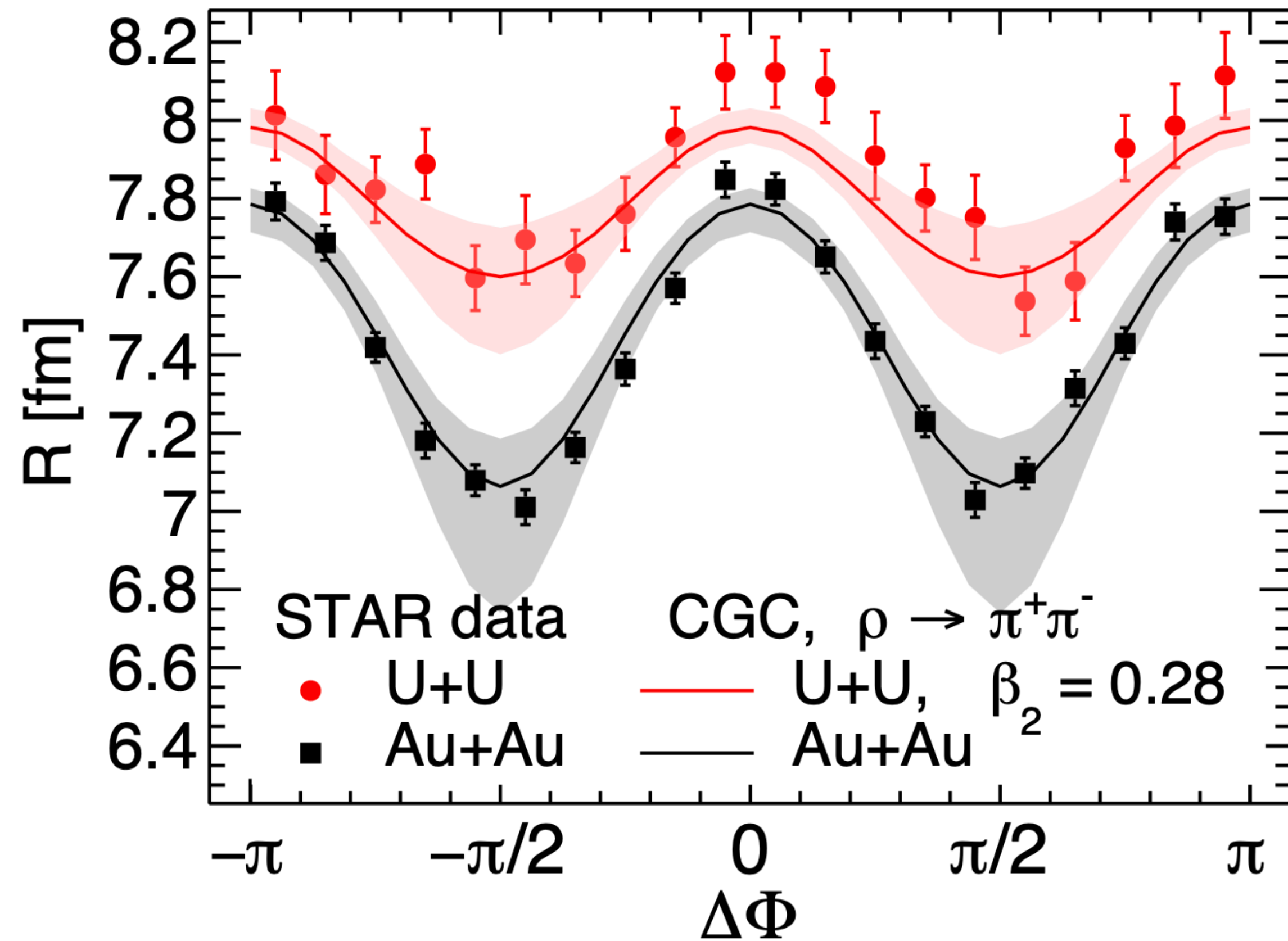
Isobar shapes - JIMWLK evolution

G. Giacalone, B. Schenke, S. Schlichting, P. Singh



Effects of nuclear radius and deformation

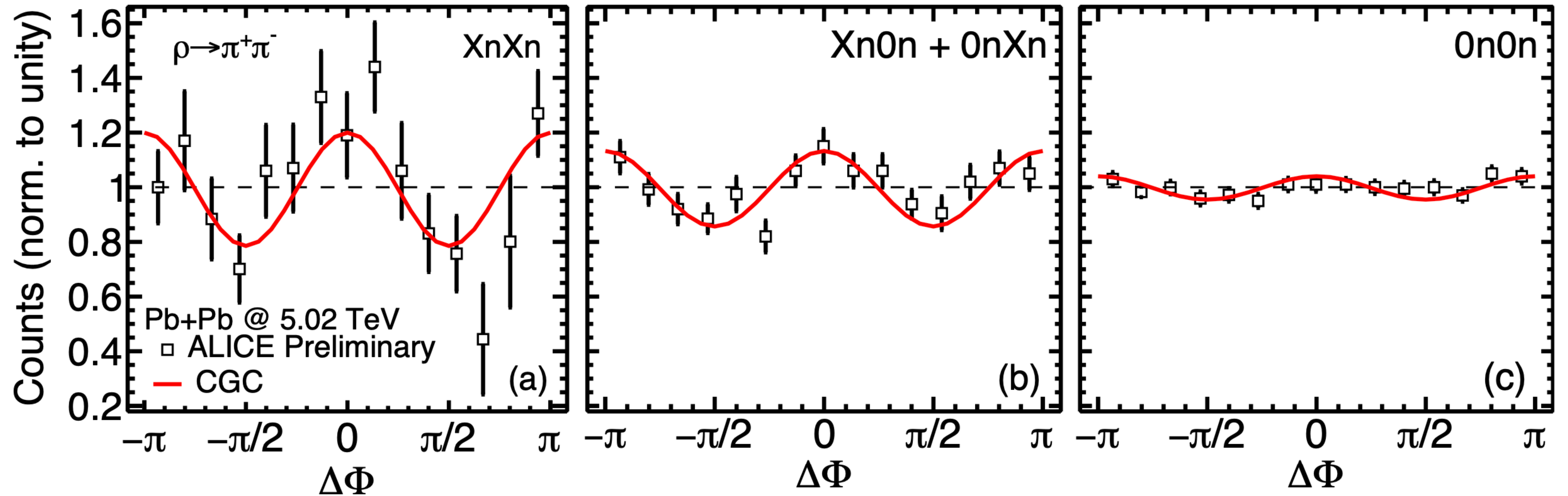
Heikki Mäntysaari, Farid Salazar, Björn Schenke, Chun Shen, Wenbin Zhao, arXiv:2310.15300



Large effect from the differences in minimal impact parameter B_{\min}

Varying impact parameter distribution at LHC

Heikki Mäntysaari, Farid Salazar, Björn Schenke, Chun Shen, Wenbin Zhao, arXiv:2310.15300



More neutrons in the forward direction prefers smaller impact parameters
Modulation decreases for larger impact parameter